



**UNIVERSIDAD DE INVESTIGACIÓN DE
TECNOLOGÍA EXPERIMENTAL YACHAY**

Escuela de Ciencias de la Tierra, Energía y Ambiente

**TÍTULO: DECIPHERING THE ACTIVE DEFORMATION
OF THE GUAYLLABAMBA DEPRESSION OF ECUADOR
USING FLUVIAL MORPHOMETRIC STUDIES**

Trabajo de integración curricular presentado como
requisito para la obtención del título de Geóloga.

Autor:

Fanny Mariela Cadena Yaguana

Tutor:

PhD. Anna Elizabeth Foster

Urququí, agosto de 2022

Urcuquí, 29 de agosto de 2022

SECRETARÍA GENERAL
ESCUELA DE CIENCIAS DE LA TIERRA, ENERGÍA Y AMBIENTE
CARRERA DE GEOLOGÍA
ACTA DE DEFENSA No. UITEY-GEO-2022-00010-AD

En la ciudad de San Miguel de Urcuquí, Provincia de Imbabura, a los 29 días del mes de agosto de 2022, a las 12:00 horas, en el Aula S_CAN de la Universidad de Investigación de Tecnología Experimental Yachay y ante el Tribunal Calificador, integrado por los docentes:

Presidente Tribunal de Defensa Dr. PINEDA ORDOÑEZ, LUIS EDUARDO, Ph.D.
Miembro No Tutor Mgs. CARLOSAMA MOREJON, FELIPE JAVIER
Tutor Dra. FOSTER ANNA ELIZABETH, Ph.D.

Se presenta el(la) señor(ita) estudiante **CADENA YAGUANA, FANNY MARIELA**, con cédula de identidad No. **1720642469**, de la **ESCUELA DE CIENCIAS DE LA TIERRA, ENERGÍA Y AMBIENTE**, de la Carrera de **GEOLOGÍA**, aprobada por el Consejo de Educación Superior (CES), mediante Resolución **RPC-SE-10-No.031-2016**, con el objeto de rendir la sustentación de su trabajo de titulación denominado: **DECIPHERING THE ACTIVE DEFORMATION OF THE GUAYLLABAMBA DEPRESSION OF ECUADOR USING FLUVIAL MORPHOMETRIC STUDIES**, previa a la obtención del título de **GEÓLOGO/A**.

El citado trabajo de titulación, fue debidamente aprobado por el(los) docente(s):

Tutor Dra. FOSTER ANNA ELIZABETH, Ph.D.

Y recibió las observaciones de los otros miembros del Tribunal Calificador, las mismas que han sido incorporadas por el(la) estudiante.

Previamente cumplidos los requisitos legales y reglamentarios, el trabajo de titulación fue sustentado por el(la) estudiante y examinado por los miembros del Tribunal Calificador. Escuchada la sustentación del trabajo de titulación, que integró la exposición de el(la) estudiante sobre el contenido de la misma y las preguntas formuladas por los miembros del Tribunal, se califica la sustentación del trabajo de titulación con las siguientes calificaciones:

Tipo	Docente	Calificación
Presidente Tribunal De Defensa	Dr. PINEDA ORDOÑEZ, LUIS EDUARDO, Ph.D.	8,6
Miembro Tribunal De Defensa	Mgs. CARLOSAMA MOREJON, FELIPE JAVIER	8,5
Tutor	Dra. FOSTER ANNA ELIZABETH, Ph.D.	9,2

Lo que da un promedio de: **8.8 (Ocho punto Ocho)**, sobre 10 (diez), equivalente a: **APROBADO**

Para constancia de lo actuado, firman los miembros del Tribunal Calificador, el/la estudiante y el/la secretario ad-hoc.



CADENA YAGUANA, FANNY MARIELA
Estudiante



Dr. PINEDA ORDOÑEZ, LUIS EDUARDO, Ph.D.
Presidente Tribunal de Defensa

Dra. FOSTER ANNA ELIZABETH, Ph.D.
Tutor



Mgs. CARLOSAMA MOREJON, FELIPE JAVIER
Miembro No Tutor



TERÁN ROSALES, ANDREA YOLANDA
Secretario Ad-hoc

AUTORÍA

Yo, **Fanny Mariela Cadena Yaguana**, con cédula de identidad 1720642469, declaro que las ideas, juicios, valoraciones, interpretaciones, consultas bibliográficas, definiciones y conceptualizaciones expuestas en el presente trabajo; así como, los procedimientos y herramientas utilizadas en la investigación, son de absoluta responsabilidad de el/la autora (a) del trabajo de integración curricular. Así mismo, me acojo a los reglamentos internos de la Universidad de Investigación de Tecnología Experimental Yachay.

Urcuquí, mes y año.

A handwritten signature in black ink that reads "Mariela Y." with a horizontal line underneath.

Fanny Mariela Cadena Yaguana

CI: 1720642469

AUTORIZACIÓN DE PUBLICACIÓN

Yo, **Fanny Mariela Cadena Yaguana**, con cédula de identidad 1720642469, cedo a la Universidad de Investigación de Tecnología Experimental Yachay, los derechos de publicación de la presente obra, sin que deba haber un reconocimiento económico por este concepto. Declaro además que el texto del presente trabajo de titulación no podrá ser cedido a ninguna empresa editorial para su publicación u otros fines, sin contar previamente con la autorización escrita de la Universidad.

Asimismo, autorizo a la Universidad que realice la digitalización y publicación de este trabajo de integración curricular en el repositorio virtual, de conformidad a lo dispuesto en el Art. 144 de la Ley Orgánica de Educación Superior

Urcuquí, agosto de 2022.



Fanny Mariela Cadena Yaguana

CI: 1720642469

DEDICATION

I dedicate this thesis to my parents, Fanny and Jesus, because their support, love, and effort were fundamental for this achievement. I also dedicate this project to my sister Ibeth; her unconditional support, love, and advice helped me through the most challenging moments of my student life because I would not have gotten here without her. Finally, I dedicate this thesis to my grandmother Celia †, from whom I lovingly keep all her advice.

Fanny Mariela Cadena Yaguana

ACKNOWLEDGMENTS

First, thanks to my co-advisor, PhD. Rafael Almeida, I express my total gratitude and admiration for his teachings, support, and patience during this work. Also, I want to thank my advisor, PhD. Anna Foster always provided me with her support and her willingness to resolve any concerns.

I am very grateful to all the School of Earth, Energy, and Environmental Sciences professors for all their academic and ethical teachings. Also, thanks to Andrea Terán, who is an important pillar of the School because with her predisposition towards the students, she has always helped us.

Finally, I thank my fellow students, especially my geo-friends Daniela, Ariana, and Jorge, with whom I shared moments of learning, unconditional support, and I enjoyed this student stage.

Fanny Mariela Cadena Yaguana

RESUMEN

La cuenca de Guayllabamba está ubicada en la zona central del Valle Interandino en la parte norte del Ecuador. La génesis de la evolución de esta cuenca aún está en estudio debido a su alta complejidad estructural. La Depresión de Guayllabamba, ubicada en la cuenca de Guayllabamba, está limitada por dos escarpes prominentes separados por el río Pisque, que los dividen en dos áreas geométricas aparentemente similares.

El análisis del área de pendiente es el método más común utilizado para analizar el perfil del río. El análisis de chi repara los errores producidos por los datos, y los resultados son mejores que los del estudio anteriormente mencionado. Para estudiar la causa de la formación de la Depresión de Guayllabamba, usamos gráficos de chi, índice de inclinación y de concavidad, los mapas de terrazas, deslizamientos de tierra y escarpes.

A partir de los resultados, observamos la diferencia significativa en el volumen de material erosionado de la Depresión de Guayllabamba con respecto a las terrazas fluviales del río Guayllabamba. Además, notamos una forma cóncava hacia arriba al inicio del perfil en el río Guayllabamba y una forma de línea recta en el resto del perfil, contraria al río Mira, que presenta una forma cóncava hacia arriba a lo largo del río. Además, observamos que no existe linealidad en los afluentes con el tallo principal, y el valor del índice de concavidad del río Guayllabamba es bajo. Nuestros resultados infieren que la cuenca de Guayllabamba es un paisaje transitorio y fue desarrollado por la erosión del río y no por condiciones tectónicas.

Palabras clave: cuenca, Guayllabamba, análisis de chi.

ABSTRACT

Guayllabamba basin is located in the central zone of the Interandean Valley in the north part of the Ecuador. The genesis of the evolution of this basin is still under study due to its high structural complexity. The Guayllabamba Depression, located on the Guayllabamba basin, is limited by two prominent scarps separated by the Pisque river, which divide them into two apparently similar geometric areas.

The slope-area analysis is the most common method used to analyze the river profile. The chi analysis repairs the errors produced by the data, and the results are better than the previous study mentioned. To study the Guayllabamba Depression formation cause, we use chi, steepness index, and concavity plots, the terraces, landslides, and scarps mapping.

From the results, we observed the significant difference in volume eroded material of the Guayllabamba Depression concerning the Fluvial terraces of the Guayllabamba river. Furthermore, we noted a concave up shape at the beginning of the profile in the Guayllabamba river and a straight line at the rest of the profile, contrary to the Mira River, which presents a concave up shape along the river. Moreover, we observed there is no linearity on the tributaries with the main stem, and the value of the concavity index to the Guayllabamba river is low. Our results infer that the Guayllabamba basin is a transient landscape and was developed by river erosion and not by tectonic conditions.

Keywords: basin, Guayllabamba, chi analysis

TABLE OF CONTENTS

1. INTRODUCTION.....	1
1.1 Hypothesis	3
1.2 Motivation for this study	4
1.3 Objectives	4
1.4 How to solve the problem?	5
2. GEOLOGIC BACKGROUND	6
2.1 Tectonics provinces of Ecuador	6
2.2 Ecuadorian Andes	7
2.2.1 Cordillera Real	7
2.2.2 Cordillera Occidental.....	8
2.2.3 Interandean Valley.....	9
2.3 Morphology of the Guayllabamba Depression	10
2.4 Previous studies of Guayllabamba basin	10
2.5 River geomorphology.....	13
2.5.1 Fluvial Terraces.....	15
2.5.2 Landslides	16
2.6 Fluvial Geomorphology Studies in Ecuador	17
3. METHODOLOGY.....	19
4. RESULTS.....	31
4.1 Landforms.....	31
4.1.1 Eroded volume & Scarps	31
4.1.2 Terraces.....	33
4.2 Fluvial morphometric analysis.....	34
4.2.1 Hydrological basins	34
4.2.2 Longitudinal river profile.....	35
4.2.3 Concavity index.....	36
4.2.4 Chi plots.....	40
4.2.5 Steepness plots.....	41
5. DISCUSSION	43
5.1 Terraces, landslides, and scarps	43
5.2 Concavity index	44

5.3 Chi analysis.....	44
5.4 Channel steepness	45
6. CONCLUSIONS	46
7. REFERENCES.....	47

INTRODUCTION

Ecuador is located at the northwest of the South American plate. The subduction of the Nazca plate beneath South America controls the Ecuadorian margin's geodynamic environment. These plates' interaction has created an active volcanic arc superposed on the Cordillera Real in the east and the Cordillera Occidental in the west with the Interandean Valley between them. (Tibaldi & Ferrari, 1992).

The Guayllabamba basin is located in the Interandean Valley of Ecuador. The formation of this valley is thought to be related to the translation of the North Andean Block, a sliver of continent moving northward (Alvarado et al., 2016; Nocquet et al., 2014). The geodynamic evolution of this North Andean Block of the South American plate has been controlled by the complex interaction of the convergent Nazca, South American, and Caribbean plates (Ego et al., 1996). The geological structures that control the tectonic development of the Interandean Valley are the Puna, Pallatanga, Cosanga and Chingual fault systems (Alvarado et al., 2016).

The aseismic Carnegie Ridge is another important piece for the geodynamics of Ecuador. It was formed by the Nazca plate's passage over the Galapagos hot spot (Gutscher et al., 1999). The Ridge is located on the Nazca plate in an east-west direction and is colliding with the South American plate (Figure 1) (Villagomez, 2003). The collision of the Ridge influences the volcanic, seismic activity, and the deformation on the Ecuadorian Andes (Gutscher et al., 1999) as well as the movement of the North Andean Block with respect to the South American plate (Villagomez, 2003).

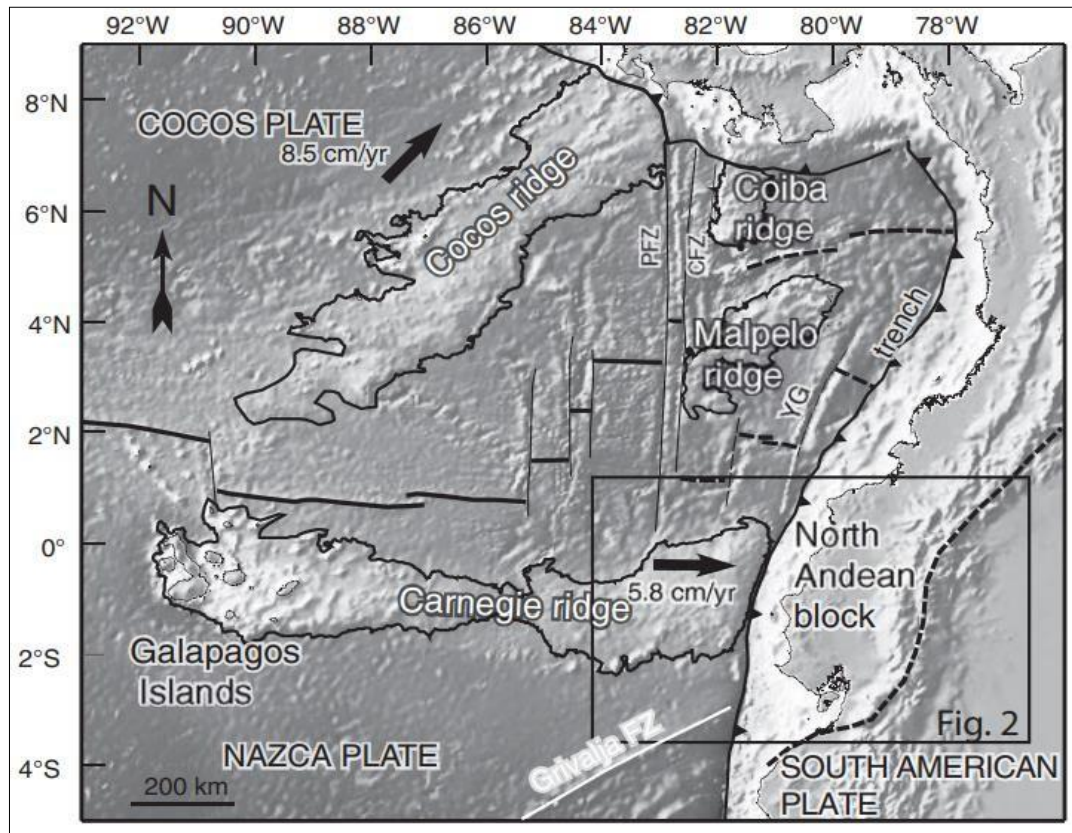


Figure 1. The geodynamic context of the Carnegie Ridge collision with the South American plate (Michaud et al., 2009).

The Guayllabamba Depression is located in the north of Ecuador, in the Pichincha province, just north of Quito (Figure 2).

The Depression is collocated with the Pliocene- Pleistocene Guayllabamba basin, which is filled with lacustrine, fluvial, deltaic, and volcanic deposits (Villagomez, 2003). The Guayllabamba Depression has generally been interpreted as a pull-apart basin controlled by a strike-slip system (Alvarado et al., 2014), and strongly influenced by the active Quito Fault System located just west of depression (Villagomez, 2003).

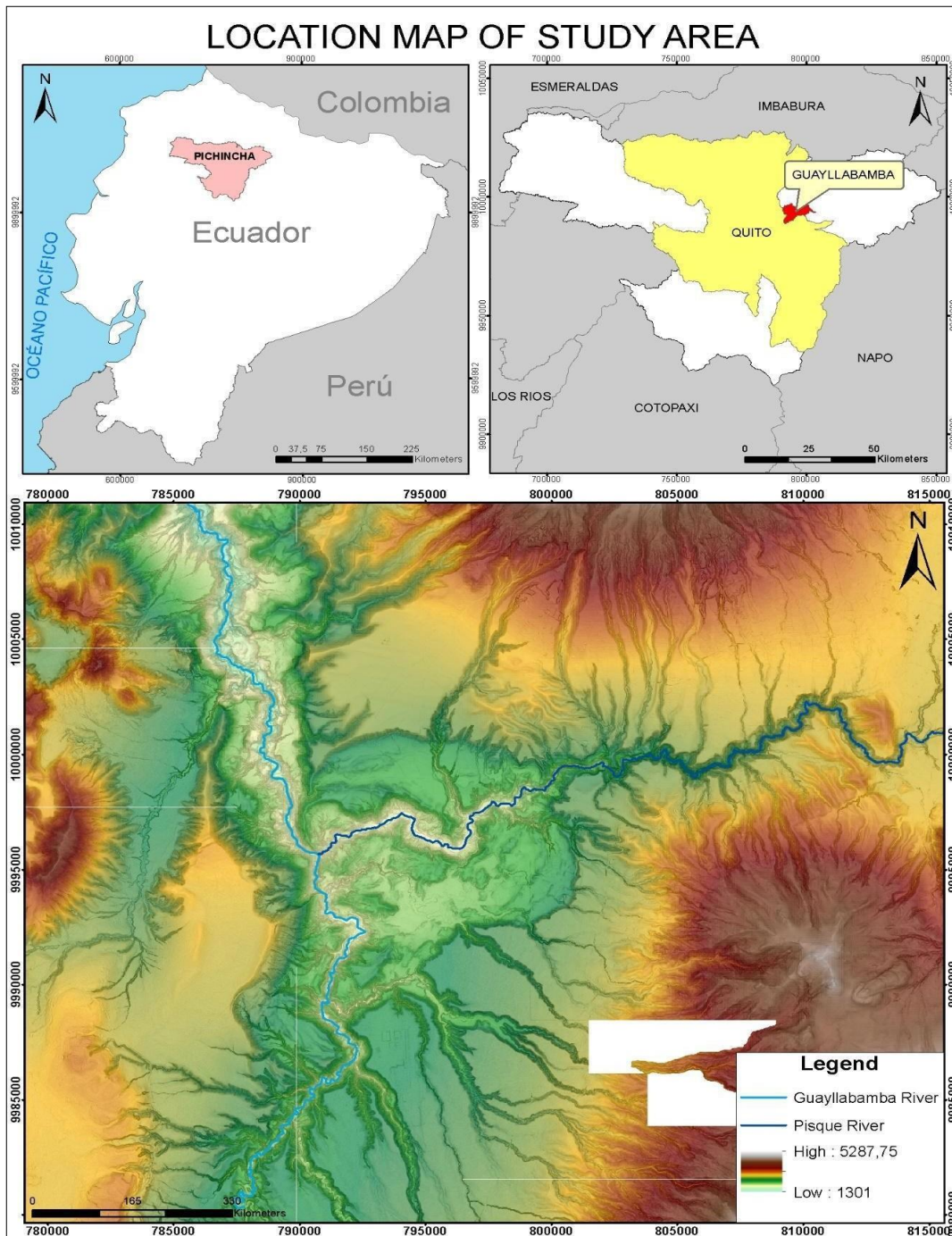


Figure 2. Location map of the Guayllabamba Depression.

1.1 Hypothesis

The present research posits that the formation of the Guayllabamba Depression is instead controlled by surface processes, in particular the deep erosional incisions produced by the Guayllabamba and Pisque rivers. These formed over steepened

canyon walls that become undercut by the rivers, which caused the collapse of the large landslides that are the dominant features in the Depression landscape. One characteristic to support this hypothesis is the geometry of the Depression, which has symmetry of the slides around the Pisque river as can be seen in Figure 2. Furthermore, we will test whether the morphology of the Guayllabamba river shows evidence of active faults across it, using state of the art quantitative fluvial geomorphological methods.

1.2 Motivation for this study

Due to Ecuador's geodynamic environment and geomorphology, this is a zone vulnerable to geological hazards such as earthquakes, volcanic eruptions and landslides. In Ecuador, there are many population settlements and infrastructure of economic importance for the country located near rivers. Therefore, the comprehension of the river effects on the landscapes can help improve the evaluation of geological hazards caused by fluvial processes such as landslides, high rates of erosion, and the obstruction of river channels by seismic activity. This research is focused on contributing to the knowledge of how the river influences the geomorphology of the surrounding area, as well as using the river morphology to better understand other elements shaping the landscape, such as active faults. The methodology applied in this research can be used in the study of any other basins. Furthermore, in this study, cutting-edge quantitative geomorphology techniques will be applied for the first time to study hydrological basins in Ecuador. Finally, the issue of whether there are active faults beneath the Guayllabamba Depression is very important to consider when estimating the seismic hazard of Quito.

1.3 Objectives

The aim of this research is to use the landscape of the Guayllabamba Depression to infer the main processes contributing to its formation. The specific objectives within this framework are:

- 1.3.1. To map the scarps, landslides, and fluvial terraces in the Depression.

- 1.3.2. To measure the total erosion caused by the Pisque and Guayllabamba rivers in the Guayllabamba Depression.
- 1.3.3. To make longitudinal profiles of the Guayllabamba and Pisque rivers and their tributaries in order to perform an analysis of chi concavity, steepness plots, and knickpoint analysis.

Finally, in this project the results of the previous analysis will be compared with the same analysis of the Mira basin (which is thought to not have widespread active deformation), to contrast the changes in results depending on if the basin is affected by active tectonic structures (Guayllabamba basin) or not (Mira basin).

1.4 How to solve the problem?

To test the hypothesis of this research and to carry out the stated objective, we will use ArcGIS and LSDTopo Tools software. Using high-resolution digital elevation models in ArcGIS, the main geomorphic features of the Guayllabamba Depression will be mapped manually. Furthermore, using the tools of ArcGIS the minimum volumes eroded by the Pisque and Guayllabamba rivers will be calculated. The fluvial morphometric analyses will be done using LSDTopo Tools, a free software developed by the Land Surface Dynamics Group at the University of Edinburgh that focuses on topographic analyses that will allow us, to make inferences about erosion and/ or uplift rates and detecting signals of divide migration.

2. GEOLOGIC BACKGROUND

2.1 Tectonics provinces of Ecuador

The convergence of the Nazca and South American plates has given rise to the formation of several tectono-stratigraphic provinces in Ecuador (Spikings et al., 2000). The tectonic provinces of Ecuador from east to west are the Oriente region or Amazon Foreland Basin, the Sub-Andean zone, the Cordillera Real, the Interandean Valley, the Cordillera Occidental, and the Coastal plain (Figure 3). The Coastal plain and the Cordillera Occidental have a basement that is formed by an allochthonous slab of oceanic crust accreted to South America during the Late Cretaceous (Aspden et al., 1988; Vallejo et al., 2009). East of the Cordillera Occidental is located the Interandean Valley, an almost continuous topographic depression, which is covered by volcanic deposits in the North part (Aspden et al., 1988), and the South part of the Valley is formed by schist, quartzite, granitic gneiss, amphibolite, cordierite gneiss, and phyllite (Aspden & Litherland, 1922). The Peltetec Fault separates the Interandean Valley from the Cordillera Real, which comprises five metamorphic terranes (Litherland et al., 1994). The Sub-Andean zone is located to the east of the Cordillera Real. In this zone, the Paleozoic to Tertiary basement and foreland basins are exposed by tectonic uplifts formed by steeply dipping thrust slices within Napo and Cutucu antiforms (Spikings et al., 2000).

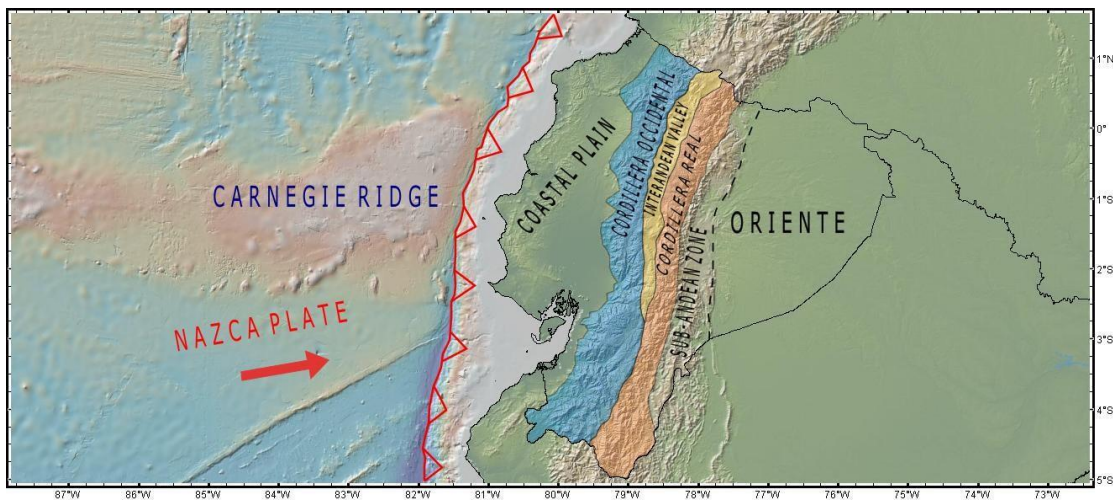


Figure 3. Map of tectonic provinces of Ecuador.

2.2 Ecuadorian Andes

The Ecuadorian Andes formed during the Mesozoic-Cenozoic in several accretionary events forming a composite orogenic belt (Spikings et al., 2000). The Ecuadorian Andes are constituted by two large mountain ranges, the oldest is the Cordillera Real and the youngest is the Cordillera Oriental. The Interandean Valley is located between them (Winkler et al., 2002).

2.2.1 Cordillera Real

This Cordillera, with an NNE direction, is composed of metamorphic rocks corresponding to autochthonous and allochthonous terrains of Paleozoic-Lower Cretaceous age (Litherland et al., 1994). The Cordillera Real has been divided into five lithotectonic divisions: Zamora, Salado, Loja, Alao, and Guamote (Figure 4) (Aspden & Litherland, 1992). The Zamora division is the eastern-most terrane of the Cordillera Real, and it is formed by calc-alkaline batholiths, andesites, dacites, basalts, conglomerates, marbles, and volcano-sedimentary rocks of Triassic to Jurassic age (Aspden & Litherland, 1992). The Salado terrane is the next division and it is formed by metasedimentary rocks, carbonate units, metamorphosed mafic volcanic rocks, and metaplutonic rocks belonging to the Jurassic-Lower Cretaceous (Litherland et al., 1994; Spikings et al., 2000). The Loja terrane is formed by metamorphosed sedimentary rocks, amphibolites, granite, and migmatite from the Triassic-Jurassic (Litherland et al., 1994; Spikings et al., 2000). Next to the Loja terrane is located the Alao terrane, which is composed of metavolcanic and metasedimentary rocks from the Jurassic. Moreover, the Alao Terrane is formed by the El Pan, Maguazo, and the Alao-Paute units (Spikings et al., 2000). The western most division is the Guamote terrane which is formed by quartzites and slates from the Jurassic-Lower Cretaceous (Spikings et al., 2000). The exhumation of the Cordillera Real occurred in different phases at different locations (Spikings et al., 2000). The main periods of exhumation are 43-30, 23-15, and 10-0 Ma, with two important pulses at ~9 and ~5 Ma (Spikings et al., 2000). Moreover, the rates of exhumation in the 43-30 and 23-15 Ma were between ~1.8-0.2 km/My, and these periods were caused by the collision of allochthonous oceanic terranes during the Eocene.

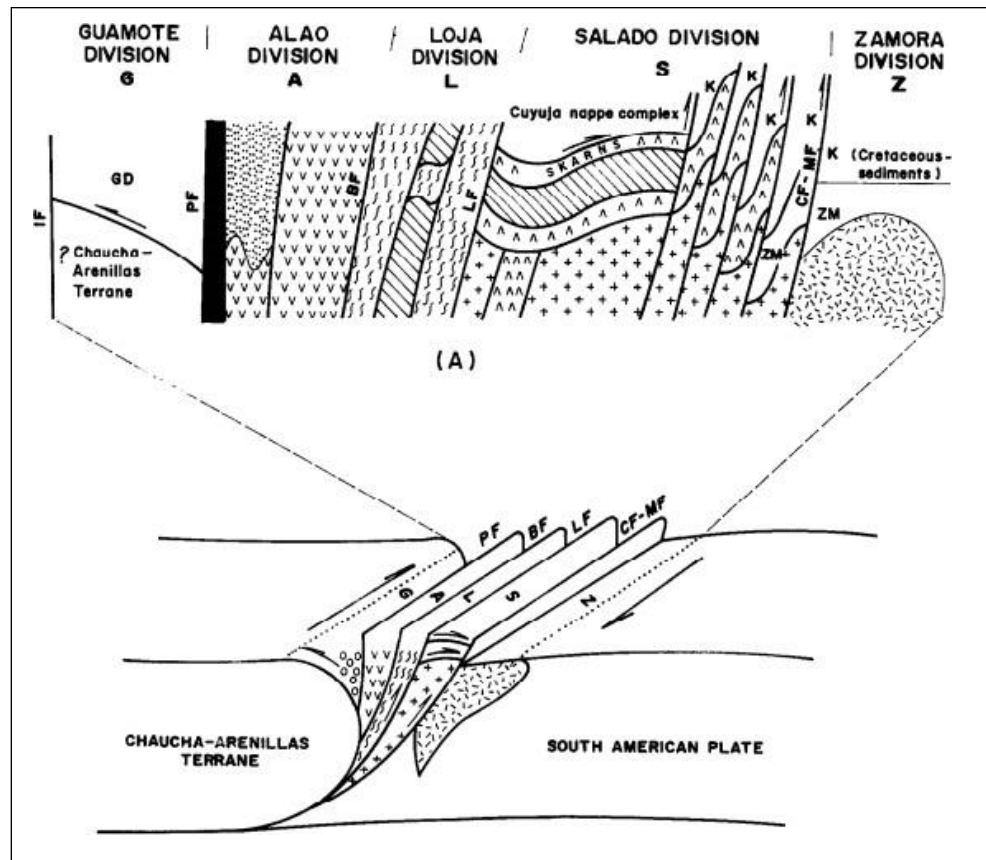


Figure 4. Schematic of the lithotectonic divisions and major faults of the Cordillera Real. PF: Pelitetec fault; BF: Baños front; LF: Llanganates fault; CF-MF: Cosanga- Mendez fault. (Aspden & Litherland, 1992).

2.2.2 Cordillera Occidental

The Cordillera Occidental constitutes the western section of the Andes mountains in Ecuador and presents a NE-SW orientation. The Cordillera is formed by allochthonous blocks of volcanic-oceanic origin (ocean plateau and island arcs) which accreted to the South American plate (Vallejo et al., 2009). The Cordillera Occidental is formed by two main terrains, Pallatanga and Macuchi. The Pallatanga terrain is the basement of the Cordillera, it is constituted by ultramafic rocks, pillow lavas, and turbidites of Cretaceous ages belonging to an oceanic plateau (Hughes & Pilatasig, 2002). The Macuchi terrain overlaps the Pallatanga terrain and is constituted by basaltic to andesitic rock composition of Eocene ages belonging to volcanic deposits of island arcs (Hughes & Pilatasig, 2002). The accretion of the Pallatanga terrain to the South American margin

began on the Late Cretaceous to Paleocene (85-60 Ma) along with the Pujili tectonic mélangé (Spikings et al., 2005). The accretion of the Macuchi terrain occurred during Late Eocene along the Chimbo-Toachi shear zone controlled by a dextral transpressive regimen (Hughes & Pilatasig, 2002). The Macuchi terrain is composed by breccias, coarse-grained turbidites, and pillow lavas (Vallejo, 2007).

2.2.3 Interandean Valley

The Interandean Valley is limited to the east by the Peltetec fault in the Cordillera Real and to the west by the Calacali-Pujili-Pallatanga fault in the Cordillera Occidental (Figure 4), and it stretches from 2°30'S in the center-south of Ecuador until the border with Colombia (Winkler et al., 2005). At the southern end of the Interandean Valley, the Calacali-Pallatanga-Pujili fault cuts across the Cordillera Occidental and eventually intersects the Ecuadorian trench in the Gulf of Guayaquil (Villagomez, 2003). For this reason, towards the South of Ecuador, the Interandean Valley has no continuation, and the Cordilleras Real and Occidental meet. The Interandean Valley is formed by several sedimentary basins from north to south, the Chota basin, Quito-San Antonio-Guayllabamba basin, Ambato-Latacunga basin, and the Riobamba-Alausi basin (Villagomez, 2003; Winkler et al., 2005). According to Winkler et al. (2002), the Interandean Valley started forming in the Late Miocene-Pliocene due to a pull-apart extension that began on the northern end and progressed to the south interpreted the Valley as a spindle-shaped pull-apart basin. Alvarado et al. (2016) proposed that the Interandean Valley has transpression and transtension zones that control the depressions and elevations due to the local faults splaying from regional faults.

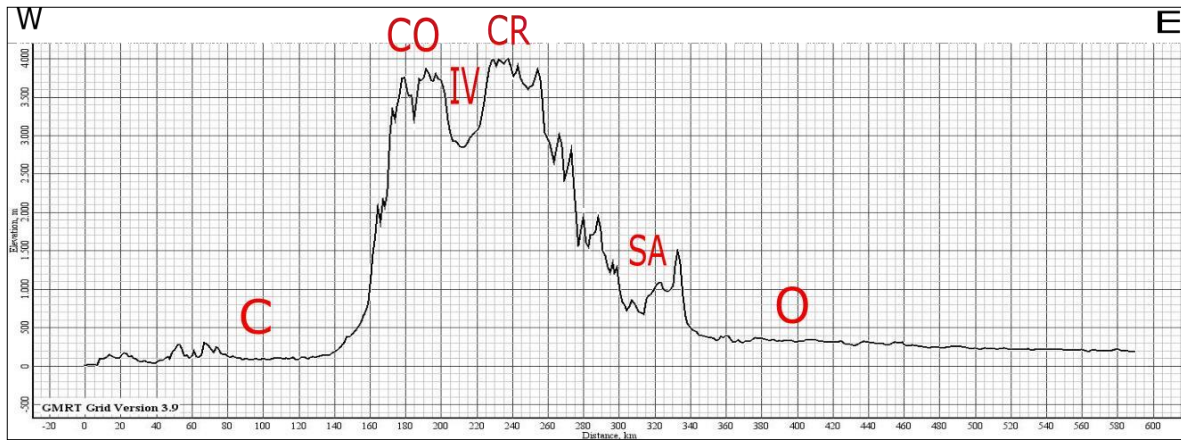


Figure 5. East-west topographic profile across a section of Ecuador at the latitude 1°00'S showing its main tectonic provinces. C: Coastal plain; CO: Cordillera Occidental; IV: Interandean Valley; CR: Cordillera Real; SA: Sub-Andean zone; O: Oriente region. Profile from Geo MapApp.

2.3 Morphology of the Guayllabamba Depression

The Guayllabamba Depression is a topographic depression characterized by having a very rugged terrain with areas of high slopes and elevations between 1850-2500 meters above sea level (Figure 2). The area coincides with the location of the Guayllabamba basin, whose fill is the product of the volcanic activity in the Ecuadorian Andes during the Plio-Quaternary (Villagomez, 2003). This area presents a dendritic drainage, alluvial landforms, several scarps, terraces, hills, and volcanic necks (Alvarado et al., 2014; Villagomez, 2003). Moreover, the borders of the basin present great altitudinal gradients and at the center, there is a considerable depression.

2.4 Previous studies of Guayllabamba basin

The formation, evolution, chronology, and structures of the Guayllabamba basin are still uncertain due to the complexity of the area. The Guayllabamba basin comprises seven geologic formations: Pisque, San Miguel, Guayllabamba, Chiche, Machangara, Mojanda, and Cangahua. The Pisque Formation (~ 200m thickness) is formed by the volcanic basement, breccias on the top, and basaltic lava on the base, likely from the Late Pliocene (Villagomez, 2003). The San Miguel Formation is formed by lacustrine, fluvial, and deltaic deposits with volcanic contributions. The

lithology of the Formation is composed of sandstones, siltstones, tuffs, and clay (Villagomez, 2003). The lacustrine deposits are strongly deformed towards the center of the Guayllabamba Depression and slightly deformed towards the edges of the Depression (Villagomez, 2003). The subsequent Formation is Guayllabamba (30-200m of thickness), which comprises volcanic and alluvial deposits: lava flows, block & ash, pyroclastic flows, and andesitic lavas (Villagomez, 2003). The Chiche Formation follows (10-100m of thickness), formed mainly by siltstones, conglomerate, andesites, rhyolites, tuffs, and fossils (Villagomez, 2003). Belonging to the Upper Pleistocene, the Machangara Formation (~100-300m thickness) is formed by pyroclastic flows, andesitic lavas, avalanches, pumice, and ash deposits, debris flows, lahars, and fluvial sands (Villagomez, 2003). The subsequent Mojanda Formation comprises the conglomerates, fluvial sands, ash, lahars, debris flows, and pyroclastic deposits. The most characteristic of this formation are two layers of white pumice coming from the Fuya-Fuya volcano (Villagomez, 2003). The last formation is the Cangahua (~20-50m thickness), consisting of yellowish to brownish tuffs intercalated with pumice, ash, and paleosoils. Furthermore, this formation presents fossils of plants, gastropods, and vertebrates (Villagomez, 2003).

There are some studies in the zone, which posit the presence of several active faults around it, which have influenced its evolution. For example, Villagomez (2003) proposes that the Guayllabamba basin is the product of a process of extension and a subsequent compression process. Furthermore, he suggests that Guayllabamba depression behaves as a pull-apart basin and that the rotational scarps collapse due to the tectonic control on the borders of the depression.

Alvarado et al. (2014) propose that convergent deformation along the north of Quito, in the Interandean Valley, is produced by two active tectonic faults, the Guayllabamba and Quito Fault Systems (Figure 6). The deformation along the reverse Quito fault system decreases to the north of the Quito region until it joins with the Guayllabamba transpressive fault system in the Guayllabamba basin, resulting in the deformation of its Plio-Quaternary volcanic deposits. Moreover, they

propose that the deformation of the area is also a product of the volcanism in the surrounding area.

Paez (2019) studied the fluvial terraces on the Guayllabamba river in three types of terraces: strath terraces (erosive with a volcanic fill), fill/ strath terraces (fluvial fill), and fill terraces (volcano-sedimentary fill). The basement of the terraces is the Pallatanga Unit and Pisque Formation. Paez proposes the distribution of the terraces shows eight phases of incision, twelve phases of fluvial activity, and four phases of accumulation as a result of the interaction of volcanism, climate, and tectonic processes. The incision phases are related to the increasing of the river flow due to climatic events or are related to increase in gradient due to the tectonic events.

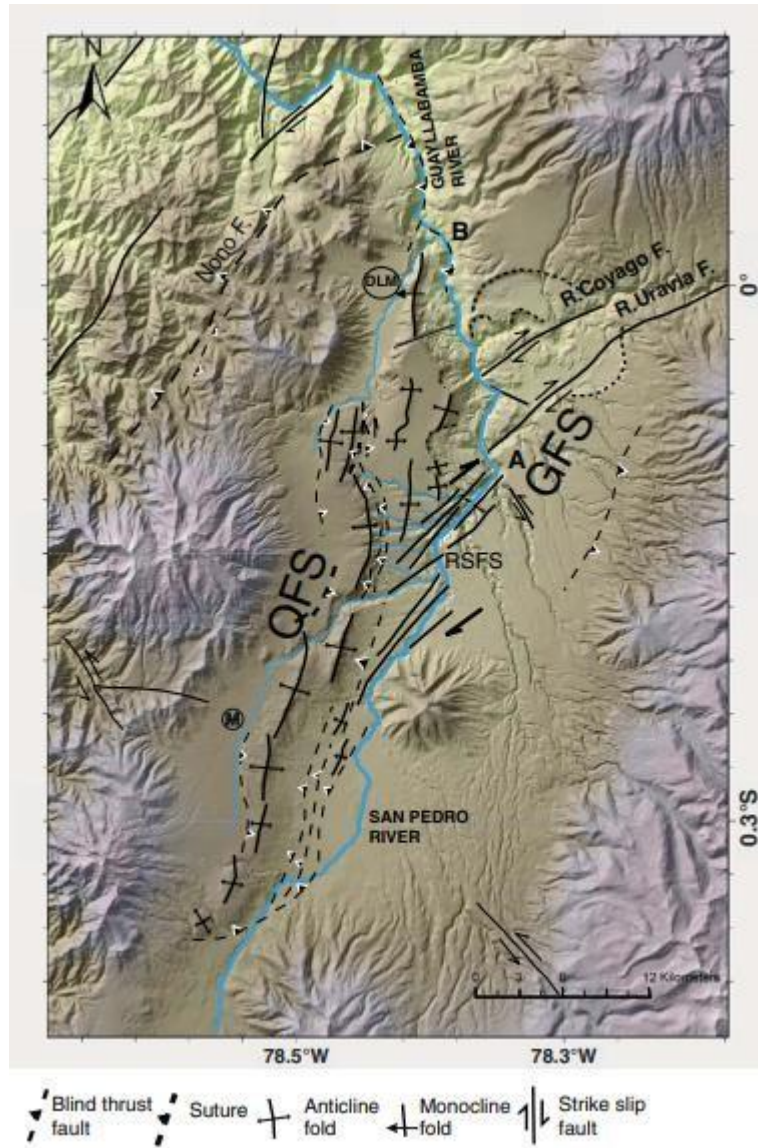


Figure 6. Fault map of Quito region. QFS: Quito Fault System, and GFS: Guayllabamba Fault System (Alvarado et al., 2014).

2.5 River geomorphology

Fluvial geomorphology studies the behavior of the rivers, their history and formation processes, and how these change the landscape (Gregory, 2000; Thorndycraft et al., 2008). Moreover, fluvial geomorphology allows for possible forecasting of changes through studies such as, numerical modelling (Thorndycraft et al., 2008). The rivers gradient, velocity and, flow, as well as external factors such

as active tectonism and, climate variations influence the river behavior, altering its morphology through erosion, weathering, and sedimentation.

The basin comprises a main stem and tributaries that drain the whole water to a river mouth. The main stem is identifiable because its length, flow, and basin area are more significant than its tributaries.

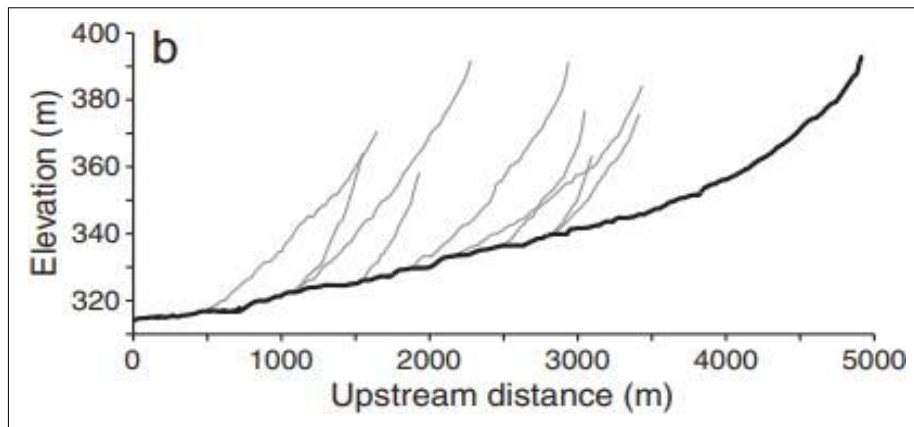


Figure 7. Longitudinal profile of the main stem (black line) and its tributaries (gray lines) of Rush Run in West Virginia (Perron & Royden, 2013).

The longitudinal profile represents a section of a river along its path from the head to the mouth (Figure 7). The typical equilibrium profile is smooth with a constant concavity, although it can present local changes (Tarbuck & Lutgens, 2005). Furthermore, the analysis of the shape of the longitudinal profile allows determining the general structure of the relief of the area's topography (Whipple et al., 2013). One of the main features to recognize in a longitudinal profile are the knickpoints (Figure 8), which represent an abrupt change in the gradient of the channel, which could be directly related to landslides, tectonism, and rock uplift (Whipple et al., 2013).

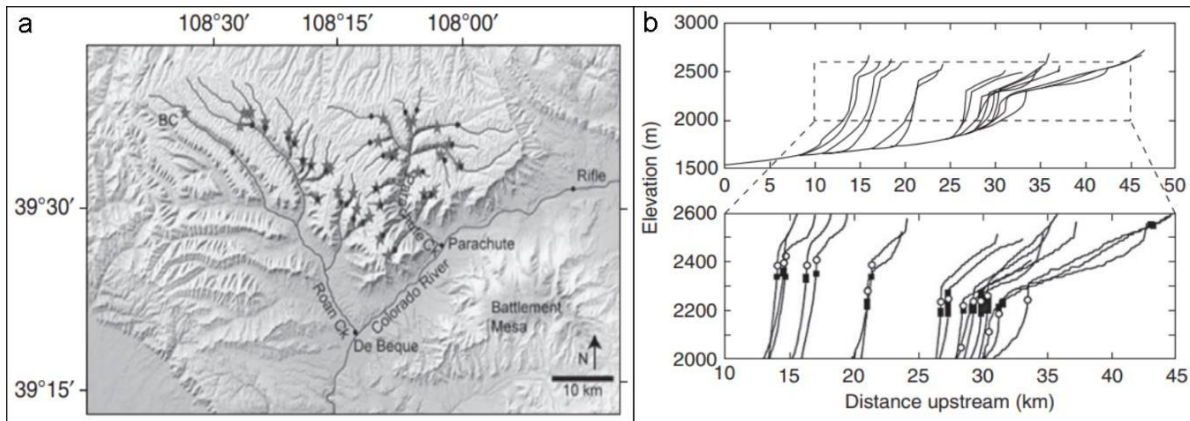


Figure 8. Graphic representation of the Roan Plateau: a) Plain view of the Roan Plateau with its main stem, tributaries and knickpoints (stars), and b) Profile of the main stem and tributaries to Parachute Creek with its knickpoints (white circles.) (Whipple et al., 2013).

2.5.1 Fluvial Terraces

Terraces are the main features of the rivers because these are a direct result of the change in elevation of the river. The terraces formation is based on the several factors that influence the change in the river flow: climatic, tectonic, and eustatic factors. The climate factor allows the river to balance its incision capacity (Paez, 2019). The tectonic factors control reactivation and change in the relief, which provokes the rising or fall of the river (Paez, 2019). Finally, the eustatic factor is related to the base level variation of the alluvial systems, and this causes the change and subsequent readjustment of the longitudinal profiles (Paez, 2019).

Fluvial incision is a fundamental geomorphic process that affects landscapes evolution (Mudd et al., 2014). One of the most widespread features formed by river incision are fluvial terraces. Fluvial terraces are geomorphologically inactive reliefs, with flat or almost flat surfaces; that have slopes between 0-5% and are ancient floodplains located at the river's course (Gutierrez, 2018). Terrace deposits are commonly composed of gravel and sand facies overlapping by finer-grained overbank facies and in some cases a basal erosional surface called a strath (Wilson et al., 2009). There are two types of terraces depending on their formation factors; these are erosional or depositional terraces (Figure 9) (Nuñez, 2011). The erosional or strath terraces have a sub-horizontal base, delimiting the

contact between the bedrock and the terrace (i.e., the strath surface). Moreover, these terraces are composed of fluvial material (Nuñez, 2011) and, are common in bedrock rivers (Whipple et al., 2013). On the other hand, the depositional terraces are composed of a thick fluvial deposit buried at the bottom of the valley; the deposit does not erode the bedrock. Furthermore, these terraces are formed by aggradation of river deposits followed by incision of the channel (Nuñez, 2011).

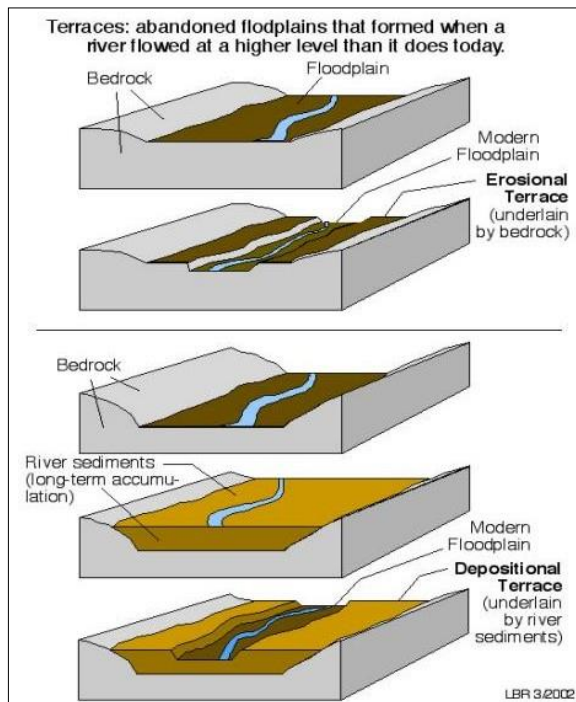


Figure 9. Erosional and depositional terraces.

2.5.2 Landslides

Landslides are important events in the interaction between the hillslopes and bedrock rivers (Whipple et al., 2013). One of the causes that trigger large landslides is the change in the slope because of vertical movement or deep erosion; the complexity of the process that leads to slope failures makes it difficult to find a clear explanation of their causes (Wilson et al., 2009). However, the relationship between fluvial incision and landslides is thought to be one of the most important factors controlling landscape evolution in mountain belts (Egholm et al., 2013). Furthermore, they are one of the most important agents

of erosion in active mountain belts, highlighting their importance for topography evolution (Korup et al., 2007). Landslides are also a factor that alters the river profiles in local areas where these are present, further emphasizing their interaction (Whipple et al., 2013). Erosion and deformation can alter the morphology of landslides after their formation; these processes influence the dynamic understanding of the landslides many times due to the lack of accurate data (Menendez et al., 2008).

2.6 Fluvial Geomorphology Studies in Ecuador

There are previous studies of fluvial geomorphology in active tectonic settings in Ecuador based on diverse forms of research. Several undergraduate theses have been done about this. Among the most relevant is Andrade (2016), which presents a study of the Rio Coca basin's geodynamic context and fluvial geomorphology. This study uses different geomorphological parameters like shape, hypsometric curve, relief, drainage, river profiles, slope, lithology, and volcanic and tectonic analysis. Andrade concludes that the Rio Coca basin presents a morphology as a result of active tectonism and fluvial processes. Moreover, the high volume of volcanic products directly affects the river's flanks because the river transports them downstream, making it highly erosive. The active tectonics in the basin is inferred from the abrupt topography, and the tectonic faults are interpreted to control the morphology of rivers. Knickpoints in the river were identified using river profiles and interpreted to be formed when active faults cross the river (Andrade, 2016).

Another relevant thesis that studies fluvial geomorphology is Ely (2017) that examines the hydro-geomorphic characterization of the Ningar River located in the paramo of the Cañar province. This study is focused on quantifying the channel geometry, describing the longitudinal characteristics of the channel, establishing its hydraulic geometry and stream-power relationships, and performing a global comparison with mountain river systems. To research the paramo river, the author used the channel geometry measurements respect to the bankfull and, substrate measurements realized on the field. Moreover, in the R software Ely analyzed the width, mean depth, velocity, boundary shear stress and discharge of bankfull, the

stream power and the critical shear stress. Moreover, along the river were observed three different streams of morphologies; riffle pool morphology, step-pool morphology, and cascade morphology. The data analysis was focused on the width, mean depth, velocity, discharge, shear stress, critical shear stress, and stream power bankfull. Ely concludes that the Ningar river is located in an active tectonic setting and not equilibrated. Moreover, the river coincides with the Rosgen classification of a non-fluvial equilibrated system.

Reyes (2018) performed a quantitative morphometric study in the Jama River, located in the Cordillera de la Costa, to detect local tectonic signals. He used two types of data for the Jama River profile analysis: to the head of the river, they used a DEM of 4m resolution, while to the downstream he used differential GPS data, and a longitudinal river profile of elevation and slope to calculate its logarithmic best fit. Moreover, Reyes performed the morphometric analysis based on the horizontal and vertical offsets of a logarithmic curve they determine as a reference of equilibrium. The results of the study show a local inflection point in the convex river profile (Figure 10), which was determined as a knickpoint, and it corresponds to the Jama Waterfalls (40 m) located at 2-4 km from the Jama fault position in the last third part of the river. Furthermore, the SL-index values indicate this change in the channel slope. Finally, Reyes concludes the relief along the Jama Range and the disturbance associated with the knickpoint point out active tectonism.

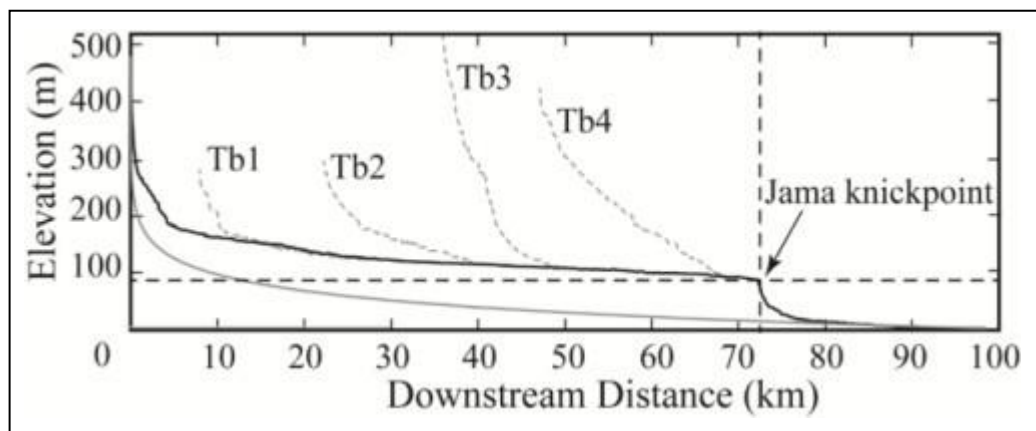


Figure 10. Jama river profile (black line), its tributaries (dashed lines), the logarithmic curve (grey line), and the knickpoint (Reyes, 2018).

METHODOLOGY

The present project was carried out mainly analyzing and evaluating information in two software, LSDTopo Tools and ArcGIS. We use LSDTopo Tools to obtain information about longitudinal river profiles, knickpoints analysis, concavity, chi profiles, and steepness plots. On the other hand, ArcGIS allows us to use digital elevation models of the terrain to identify the fluvial terraces and scarps in the Guayllabamba Depression and calculate eroded volumes.

Bedrock rivers are rock-bound; the banks and bed are composed almost completely of in situ bedrock (Whipple et al., 2013). These record information of lithology, climate history, tectonic context, and landscape bedrock (Perron & Royden, 2013). The most common models used to study bedrock river incision are focused on expressing the erosion rates as a function of channel slope and drainage area. This is based on steady-state conditions, which is defined by Whipple et al (2013) as follows, “steady-state refers to a condition in which the channel profile has fully adjusted to the climatic, lithological, and tectonic conditions imposed upon it”. These factors need to be invariable over long periods of time to give the river the necessary time to adjust its longitudinal profile to the prevailing conditions; these factors don't need to be uniform in space (Whipple et al., 2013).

The bedrock river profiles have been interpreted mostly with slope-area analysis. This analysis is easily applied to the landscape evolution models, topographic measures, and deduce of tectonic and erosion events (Perron & Royden, 2013; Wobus et al 2006). Unfortunately, slope-area method presents some errors that complicate their use for analysis of bedrock rivers, such as the noise, gaps and uncertainty in the topographic data due to local variations on the slope registered on the DEM (Perron & Royden, 2013; Whipple et al., 2013, Wobus et al., 2006). These errors introduce spurious values that affect the identification in the subtler temporal and/ or spatial variations in the erosion rates, knickpoints related to the landslides, and rock strength (Perron & Royden, 2013; Whipple et al., 2013). According to Wobus et al. (2006) to use the slope-area method, first, it is necessary to smooth the DEM. Next, the topographic gradient is measured over a stable drop in elevation or a stable reach length, and finally, the data are averaged over logarithm spaced bins.

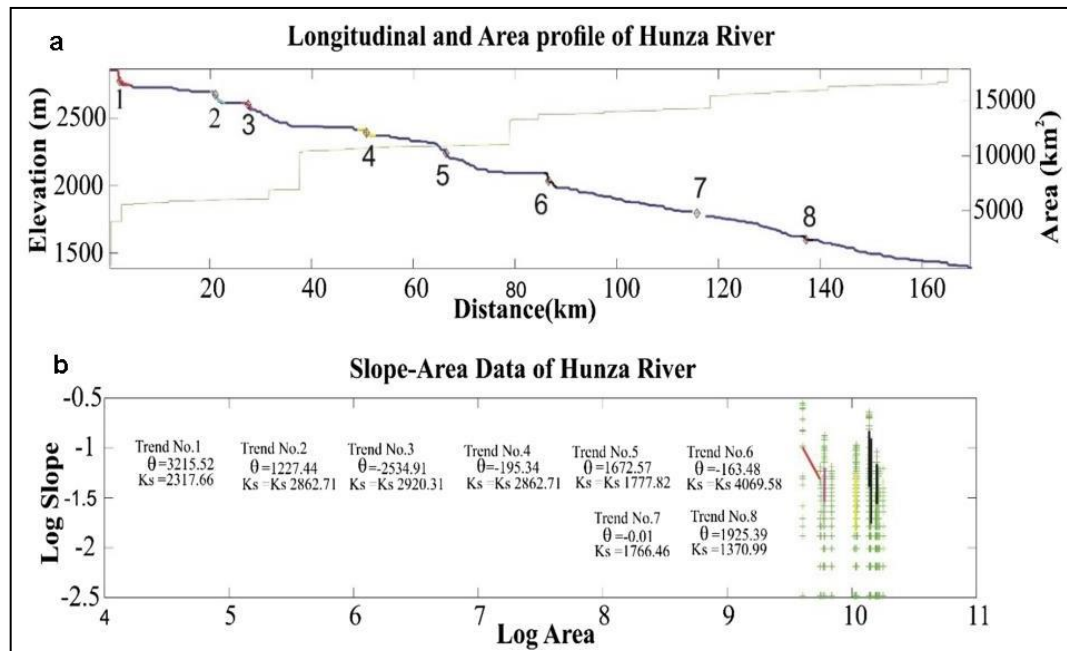


Figure 11. Graph of the longitudinal profile (black line) of the Hunza River, Pakistan that shows: a) the knickpoints along the river marked with the number, and b) the variation of steepness index K_s and channel concavity θ at different areas (Ahmed et al., 2019).

Due to these issues, here we use the chi analysis method developed by Perron and Royden (2013), which can be applied to bedrock rivers in steady-state or not. The chi (χ) analysis extracts information from channel profiles and then compares tributaries or main stems with different discharges or tributaries, as a function of elevation (Mudd, Clubb & Gailleton, 2018).

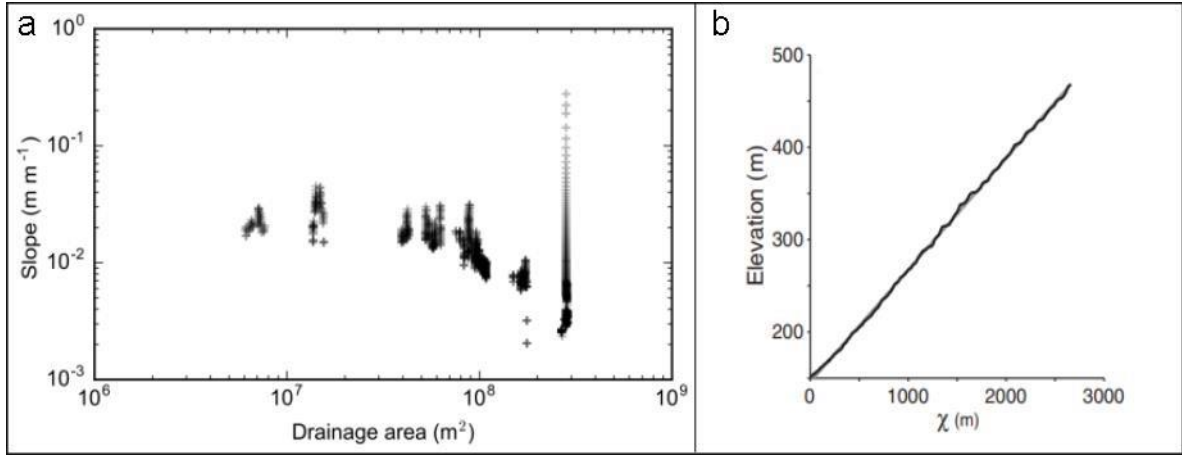


Fig 12. Comparison between a) slope-area plot and b) chi method analysis (Perron & Royden, 2013; Mudd et al., 2018).

This method reduces the errors previously mentioned by integrating the horizontal coordinate of the river profile. The integration method starts from the equation of the stream power model:

$$\frac{\partial z}{\partial t} = U(x, t) - K(x, t)A(x, t)^m \left| \frac{\partial z}{\partial x} \right|^n \quad (1)$$

Where z is the elevation of the channel (dimensions length), t is time, x is the horizontal upstream distance, U is the rate of rock uplift, K is the erodibility coefficient, A is the drainage area, and m and n are constants (empirically derived) (Mudd et al., 2014; Perron & Royden, 2013). If the study is based on a topographic steady-state, where erosion equals uplift and therefore there is no change in the topography and $\partial z/\partial t = 0$, with uniform K and U , then the equation simplifies to:

$$\left| \frac{dz}{dx} \right| = \left(\frac{U}{K} \right)^{\frac{1}{n}} A(x)^{-\frac{m}{n}} \quad (2)$$

To change the horizontal coordinate to a function of chi, and to have length units in both axes, it is necessary to integrate Equation 2 in the upstream direction from a base level x_b and add a reference drainage area (A_0) (Perron & Royden, 2013):

$$z(x) = z(x_b) + \left(\frac{U}{KA_0^m} \right)^{\frac{1}{n}} \chi \quad (3)$$

$$\chi = \int_{xb}^x \left(\frac{A_o}{A(x)} \right)^{\frac{m}{n}} dx \quad (4)$$

Eq. 3 forms a line in chi-z space where z is the “y” axis (dependent variable) and the χ represent the “x” axis (independent variable) both in distance units, and the slope of the lines is $\left(\frac{U}{KA_o^m} \right)^{\frac{1}{n}}$ (Perron & Royden, 2013). In Eq. 4 we can see that χ depends on the m/n ratio, which is referred to as the concavity index or the channel concavity. It describes how concave the profile is (Mudd et al., 2014; Mudd et al., 2018).

To identify the best m/n ratio for a drainage system, i.e., the one that best linearizes the data, it is calculated iteratively within a range of values, and the one that maximizes the R^2 value of the data in chi-z space is selected. Since we assume that the properties of the drainage basin are the same throughout, the calculation must be made for the main stem and for its tributaries (Mudd et al., 2014). Thus, the correct m/n ratio must collapse the main stem and all its tributaries in a single line and linearize all profiles (Figure 13) (Mudd et al., 2014; Perron & Royden., 2013).

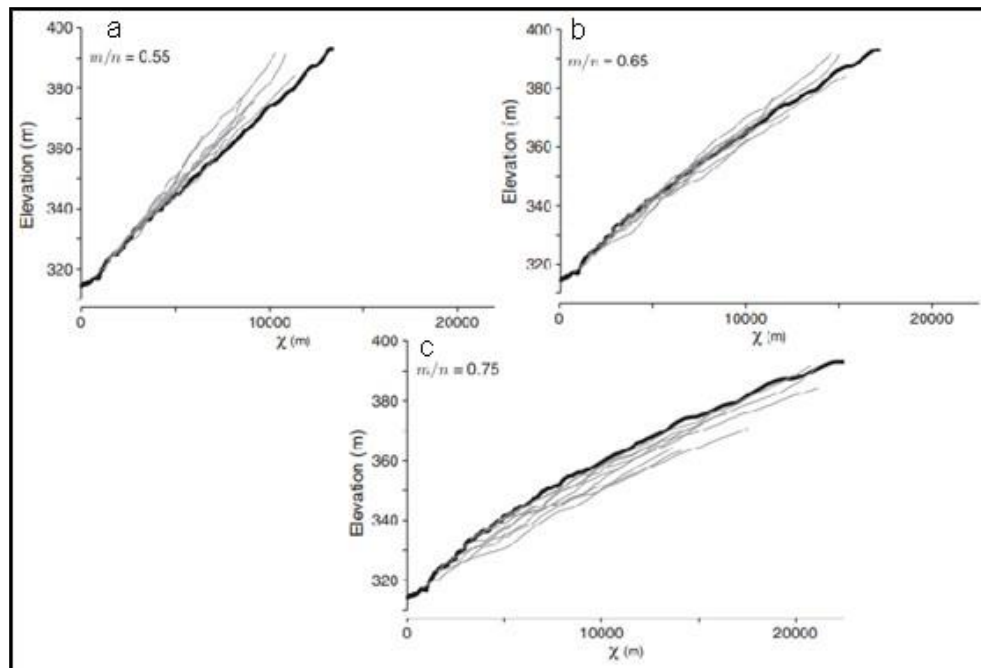


Figure 13. Chi plots of longitudinal profiles showing how the best choice of m/n changes the tributaries with respect to the main stem. (a) The tributaries

have a higher elevation than the main stem. (c) The tributaries have a lower elevation than the main stem. (b) The best choice of m/n collapses the tributaries and the main stem (Perron & Royden, 2013).

The correct value of the concavity index is important to be able to obtain the correct steepness index since the higher the value of the concavity index, the faster the downstream channel gradient decreases (Mudd et al., 2018). Perron & Royden (2013) proposed a method to calculate the concavity index, the method searches for the collinearity of the tributaries with the main stem.

Mudd et al. (2018) propose the chi disorder method to select the best m/n value. This statistic analysis is based on each complete channel network taking the first chi-elevation pairs of each point, ordered by increasing elevation. Mudd use the Eq 5 to calculate the sum:

$$S = \sum_{i=1}^N |X_{s, i+1} - X_{s, i}|, \quad (5)$$

Where the s, i is the i th chi coordinate, the S is minimal if the chi and elevation are related monotonically, it's sensitive to change because of the concavity index. To realize this process, the software, first, take a combination of three tributaries with the main stem in the basin to then iterate through a concavity indices range to calculate the chi disorder metric (Mudd et al., 2018). This process allows to find the best concavity index which minimizes the disorder to each combination, and giving a several concavities with the best fit (Mudd et al., 2018).

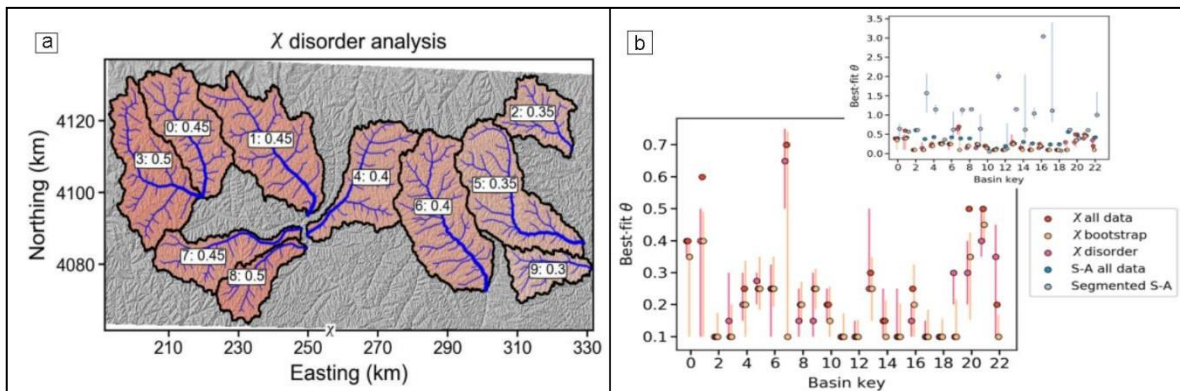


Figure 14. Best fit concavity indices in the basins in the Loess Plateau, China. (a) Plot raster

showing the best fit concavity of each basin based on chi disorder analysis. (b) Plot using the slope-area analysis (blue points), and chi analysis (red points) (Mudd et al., 2018).

The steepness index is related to the erodibility (K) and uplift rate (U) parameters, and it establishes the gradient of the channel (Mudd et al., 2018). In Equation 2, $(U/K)^{1/n}$ is the steepness index, and is related to the intersection of a linear fit to the area and slope data in logarithmic space (Perron & Royden, 2013). Furthermore, the integral method in the steepness index reduces the uncertainty, making it possible to better analyze the channel networks (Mudd et al., 2014; Perron & Royden, 2013).

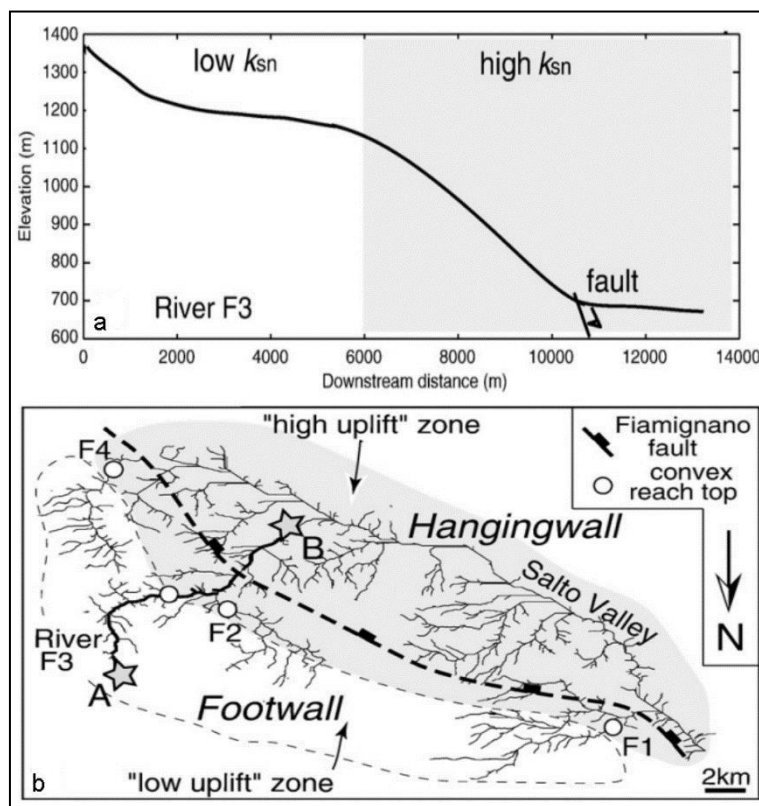


Figure 15. Graph shows the relation between tectonic uplift and the steepness index K_{sn} (b) of a river crossing an active normal fault in the Apennines of Italy (a) (Whittaker et al., 2008).

Mountain streams usually have knickpoints, which are locally steep and convex-upward (Figure 16). These knickpoints can form at locations where the uplift rate (U) or erodibility (K) varies, and will travel at a constant vertical celerity. In addition, the

knickpoints affect the calculation of the concavity index because incision rates are different below and above these points (Niemann et al., 2001).

Mudd et al. (2018) used collinearity to relate the concavity index of the channel with the knickpoints propagation in space. This can be used in transient landscapes by comparing all elevation tributaries data with the main stem.

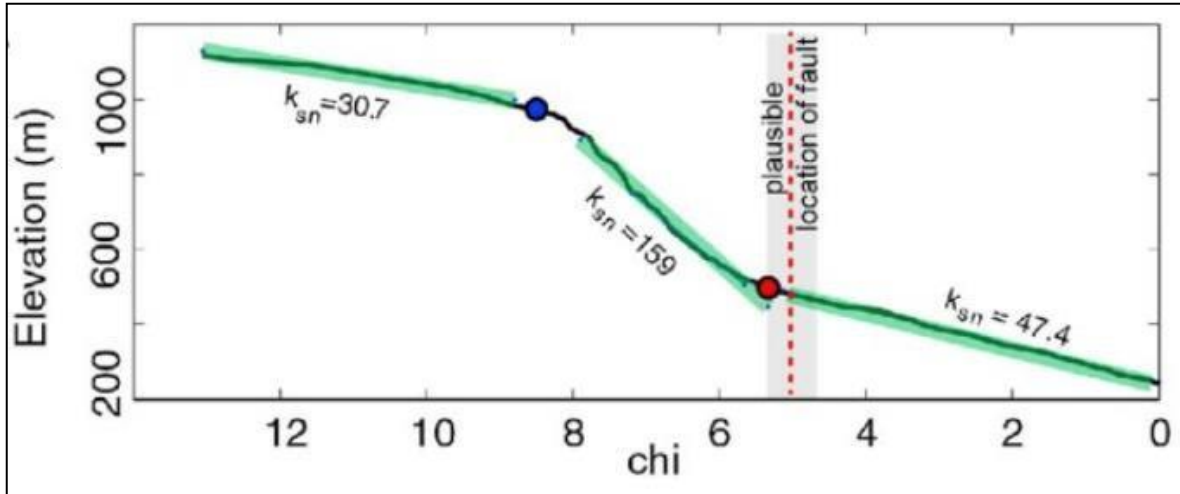


Figure 16. Graph of a chi plot showing the relation between knickpoints (blue and red dots) location and steepness index (K_{sn}) changes of a catchment crossing a reverse Cimandiri fault zones on the West Java, Indonesia (Marliyani et al., 2016).

Mudd et al. (2018) proposed the horizontal celerity equation in length per time:

$$Ceh = \frac{1}{S_2 - S_1} \Delta E \quad (6)$$

Where S_1 and S_2 are the channel slope prior and after disturbance, respectively, and the ΔE is the difference before and after in the incision rate, it is possible to equal the uplift rates with the incision rates. Eq.6 was inserted into the power law; therefore, the concavity index is independent of the uplift rate, and the horizontal celerity is a function of drainage area:

$$Ceh = \frac{U_2 - U_1}{K_{s2} - K_{s1}} A^\theta \quad (7)$$

In this research, we use LSDTopo Tools, to analyze the concavity index, steepness index, and knickpoints of the Guayllabamba and Mira rivers using the chi method. We compare results obtained using two types of Digital Elevation Model data. The first DEM used is from the Shuttle Radar Topographic Mission (SRTM) and it is used for the Mira basin. The SRTM data is in the WGS84 coordinate system and has 30 m resolution. The second data used is from the Ministerio de Agricultura of Ecuador, with 3, 5, and 10 m of the resolution, which we interpolated to obtain a uniform 3 m of resolution. The coordinate system of this data was SIRGAS, which we changed to WGS-84. The difference between the two types of DEM is shown in Figure 17.

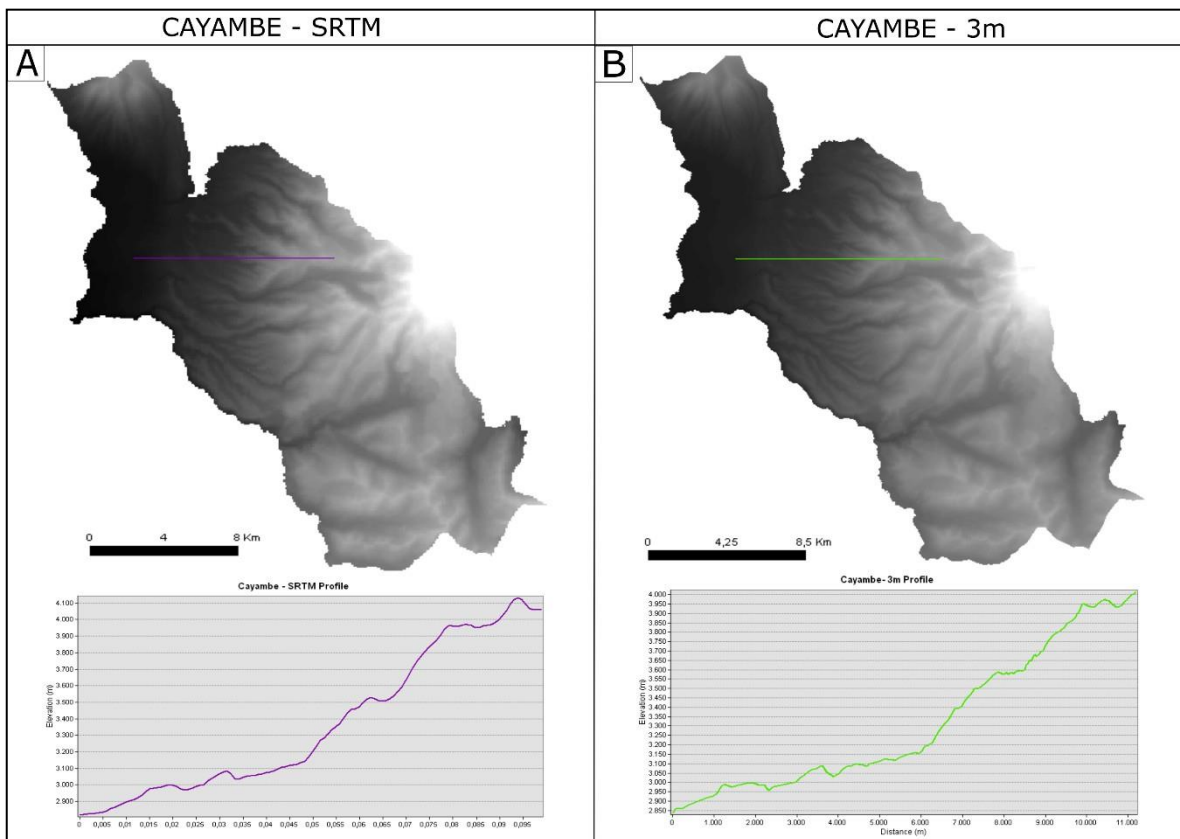


Figure 17. Comparison figure of the quality of the DEMs. A: DEM and profile of Cayambe with SRTM data; B: DEM and profile of Cayambe with the data of Ministerio de Agricultura.

To prepare the DEMs for the LSDTopo Tools and ArcGIS analysis, first, we obtain the data in tiff version, and then to fill the gaps within the 3 m DEM we go through the following steps in ArcGIS:

1. First, in ArcMap, we upload all tiffs that cover the area of interest. We use the tool Mosaic to New Raster and the tool Extract by Mask to select the area of the Basin (Figure 18).

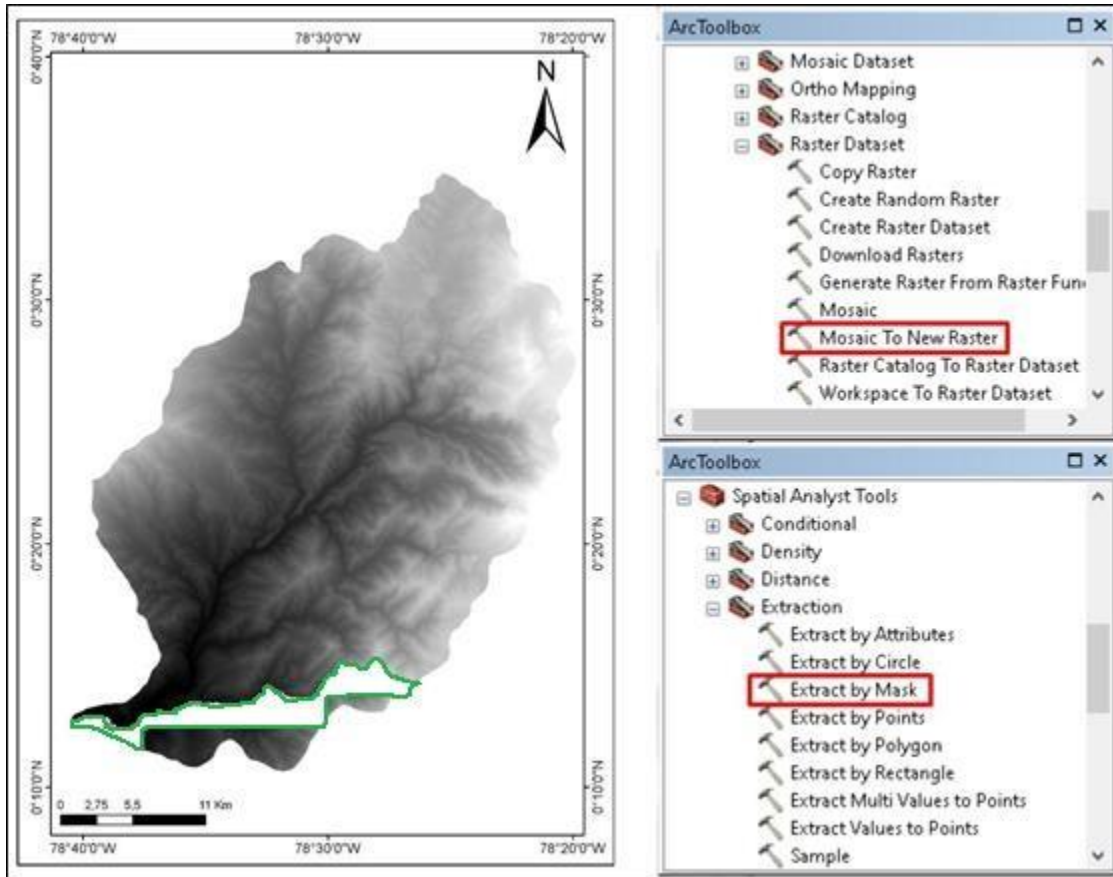


Figure 18. Part of the Guayllabamba Basin using Mosaic to New Raster and Extract by Mask tools. Green polygon represents the gap to fill with SRTM data.

2. Second, we made a clip of SRTM map of Ecuador to extract the area of interest. Then we interpolate the cell size to 3m using the Export Data function in ArcMap.

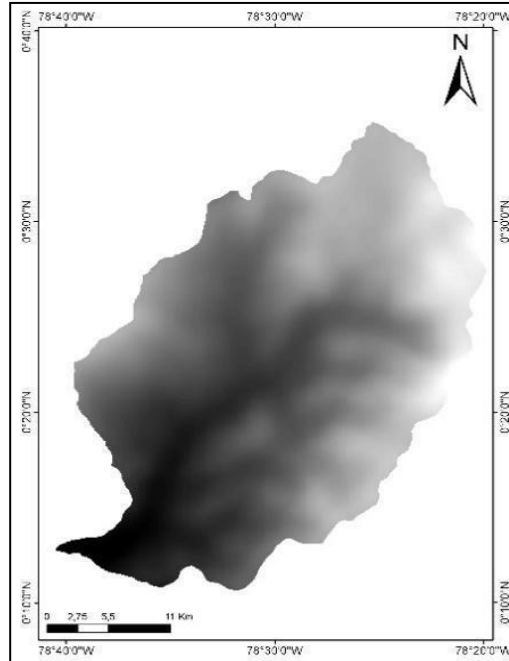


Figure 19. The area in SRTM data with 3m of cell size.

3. Finally, we use the Raster Calculator tool to fill the data without values with the interpolated data of the SRTM.

To map the topographic features in the Guayllabamba basin, we use the 3m DEM using the following steps in ArcMap:

1. We make an adjustment of the DEM, selecting the zone where the Guayllabamba Depression is located. (Data Management Tool → Raster → Raster Processing → **Clip**) (Figure 20).

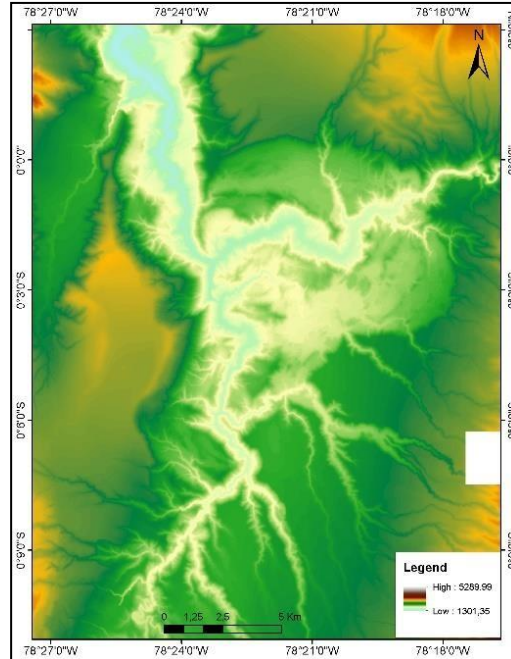


Figure 20. DEM of Guayllabamba Depression.

2. Then, we make a slope map to enhance the relief of the zone. (Spatial Analyst Tool → Surface → Slope) (Figure 21).

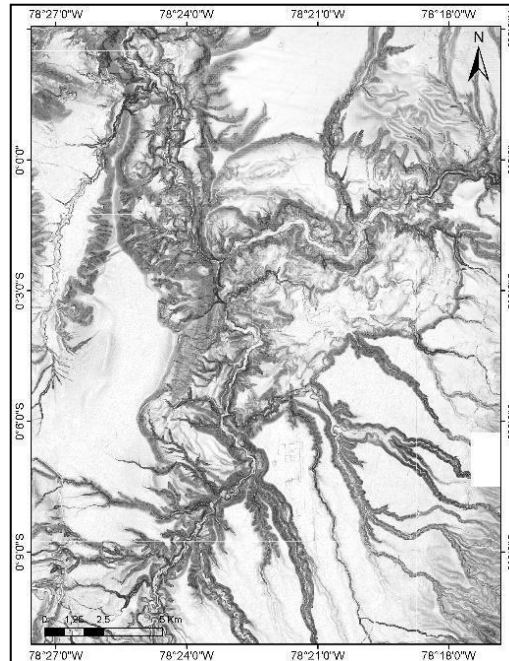


Figure 21. Slope map of the study area.

3. Finally, we overlap the slope map over the DEM with a 60% transparency to start the visual recognition of the scarps, before and after the erosion, and the terraces of the Guayllabamba river.

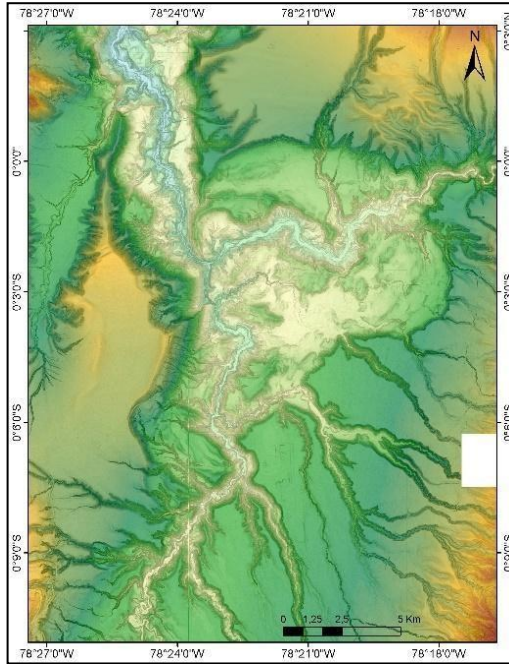


Figure 22. Final Guayllabamba DEM overlapping Fig 20 and 21

4. The identification of terraces and scarps was carried out by drawing polygons over the slope map and the DEM. The recognition of these features was assisted by also using Google Earth.

4. RESULTS

From analyses in both software LSD TopoTools and ArcGIS, we obtain the following results for the Mira and Guayllabamba basins.

4.1 Landforms

We use the ArcMap GIS software to identify and analyze several types of landforms in the Guayllabamba basin.

4.1.1 Eroded volume & Scarps

The volume of eroded material from the river valleys of the Guayllabamba Depression is of approximately 500,722 Km³ (Figure 23). This volume was calculated assuming that the plain terraces that form upper surfaces of the Guayllabamba Depression were continuous across the Depression prior to incision of the Pisque and Guayllabamba rivers.

We have also mapped the landslide scarps (Figure 23b) of the Guayllabamba Depression that delimit it and give it's the characteristic geometry. The bottom of the scarps is colored in red, and the top of the scarps are colored in purple. The arcuate nature of these scarps leads us to interpret them as the head scarps of rotational landslides.

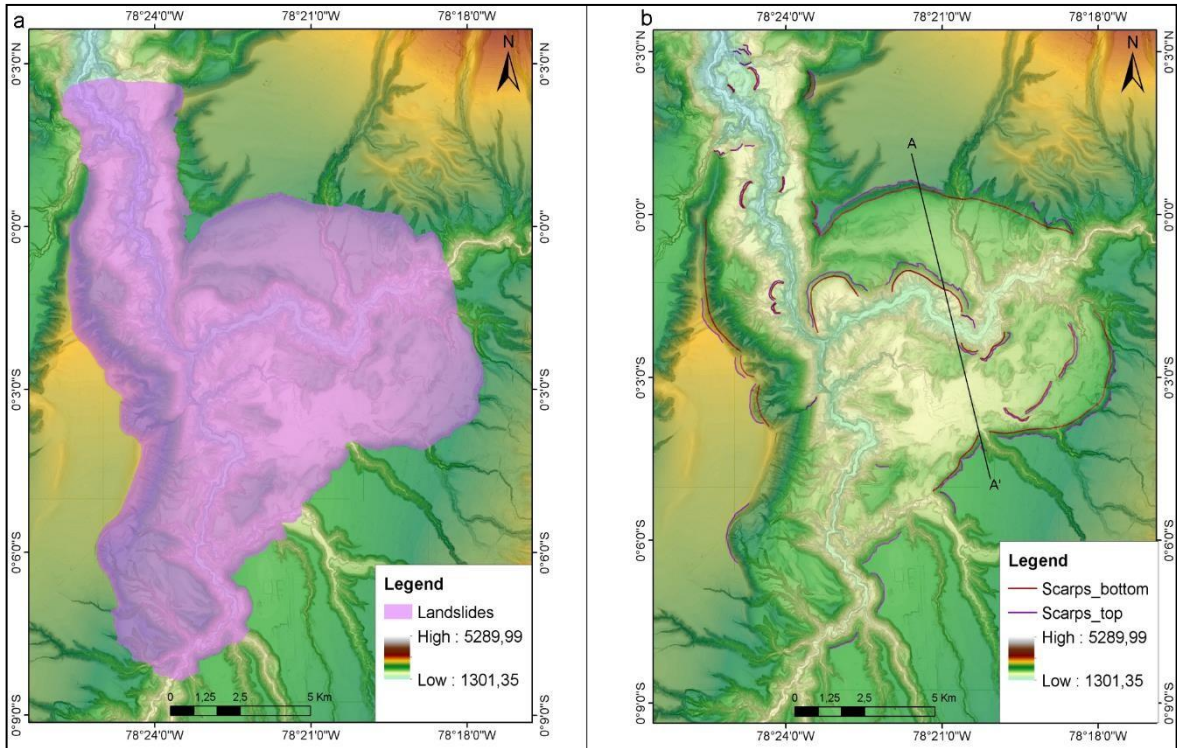


Figure 23. Map of the eroded volume of the Guayllabamba Depression showing: (a) area of eroded volume and (b) the bottom (red) and top (purple) of the scarps. Location of the cross-section in Fig. 24 shown as black line.

The cross-section of the Guayllabamba Basin shows that the north part of the basin is almost 100m higher than the south part, this probably occurs by the preexisting topography of the flanks of the volcano. Moreover, the river is more or less centered in the depression, being only slightly shifted to the south (although since the river meanders, this distance varies).

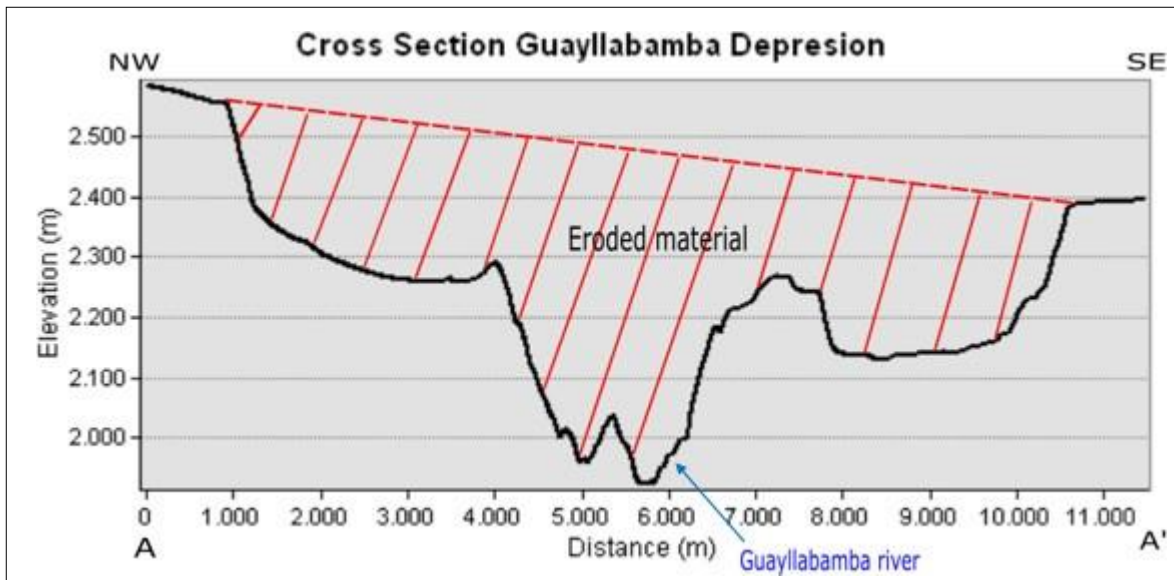


Figure 24. Cross section of the Guayllabamba Depression showing the eroded material (red lines).

4.1.2 Terraces

Along the Guayllabamba and Pisque rivers, inside of the Guayllabamba Depression Fluvial and Plain terraces were identified (Figure 25). The plain terraces are the oldest and largest features, and are located at higher elevation, while the fluvial terraces are the younger, smaller features, and are located at lower elevation. The plain terraces are formed by material coming of volcanic edifices and form landscape into which the Pisque and Guayllabamba rivers are incised. The fluvial terraces form as the base level of these rivers fluctuates within their present canyon. There are 124 fluvial terraces developed on both sides of the rivers and 36 plain terraces. The volume of the fluvial terraces is 29,506. The plain terraces inside the depression were part of the original surface and were displaced by the scarps, but these surfaces were continuous.

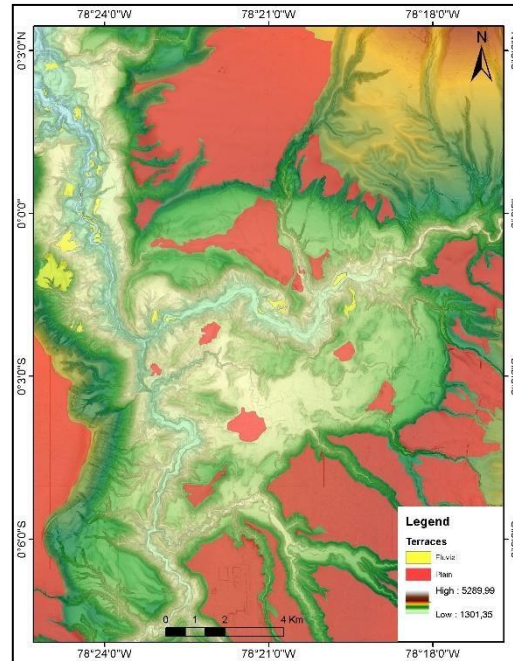


Figure 25. Terraces distribution on the Guayllabamba Depression, Fluvial terraces (yellow) and Plain terraces (red).

From these results we can see that the amount of material that has been removed by erosion is much greater than the sediment stored in the river system as fluvial terraces. This shows that the amount of material removed from the Guayllabamba Depression is much greater than that stored throughout the system.

4.2 Fluvial morphometric analysis

4.2.1 Hydrological basins

In order to analyze the fluvial profiles of the Guayllabamba and Mira basins we use the LSD TopoTools software. The first step is to, carry out the basin selection to determine the extent of the Guayllabamba and Mira basins (Figure 26). The software determines the drainage network of each of the basins. Fig 26 shows all drainages with a minimum drainage area of 3500 pixels. The area of Guayllabamba basin is 8223 Km² and the area of the Mira basin is 6555 Km². Each point corresponds to the intersection of two rivers. The yellow points represent the river's intersection in the Mira basin, and the blue points

correspond to the river's intersection in the Guayllabamba basin. The start point of the river's distance being on the fluvial fans.

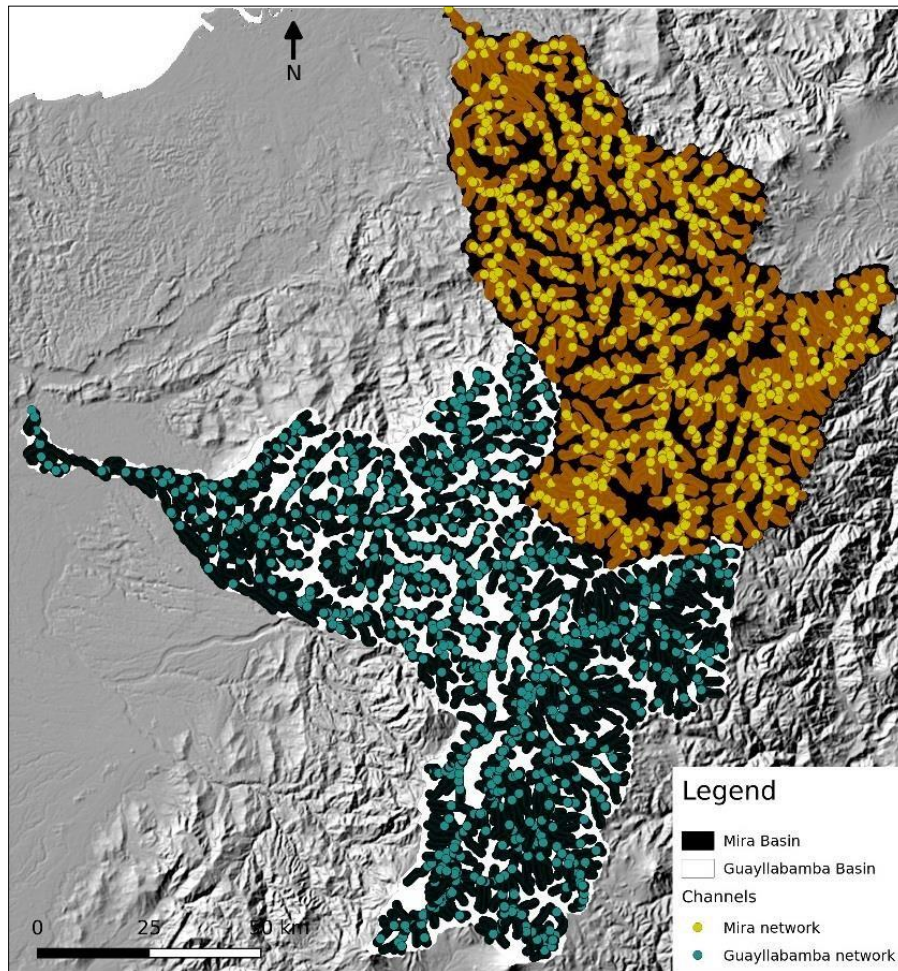


Figure 26. Guayllabamba (a), and Mira basins over a hillshade map, UTM zone 17S.

4.2.2 Longitudinal river profile

In Fig. 27 we show the longitudinal profiles of the main stem and tributaries in each basin as well as the drainage network maps of the Guayllabamba and Mira basins colored based on their source.

The Guayllabamba profile shows two tributaries colored in brown on the 150-200 km distance with a clear change on their steepness. In the Mira longitudinal profile, an area located at 140-190 km is clearly concave up, and then the river profile continues normally.

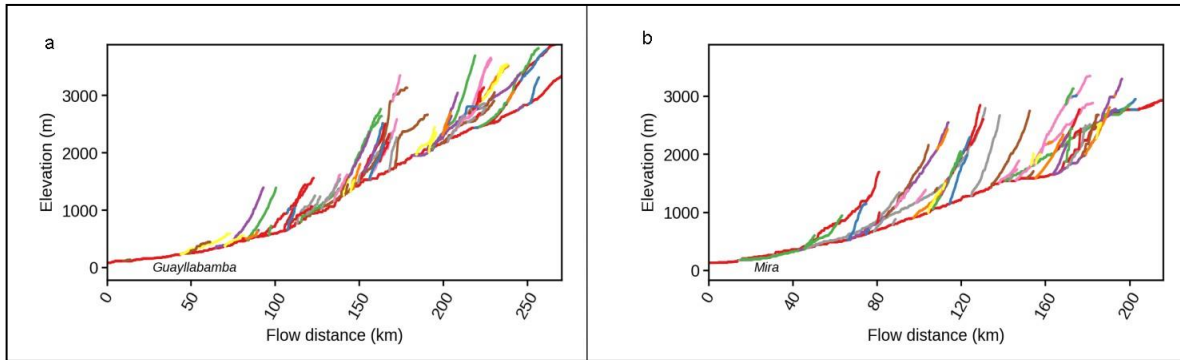


Figure 27. Longitudinal profiles of the a) Guayllabamba and b) Mira basins.

4.2.3 Concavity index

One of the most important parameter to be able to calculate the chi parameter (Figure 32) we must determine the concavity index. To do this we employ the chi disorder statistic and the best fit concavity. Moreover, the result of these methods was compared with the result of the traditional slope-area method.

4.2.3.1 Guayllabamba basin

The chi disorder statistic method to Guayllabamba basin gives a result of 0.3 (Figure 28a). Figure 28b shows the gaps, due to abrupt increases in the area of the basin, that tributary junctions produce in the slope-area method. Moreover, the wide ranges due to the noise in the data which derives from slope values. The best comparison between the methods to obtain the concavity is shown in Figure 28d, where the chi disorder method is defined for a red point, and its concavity is 0.3. In Figure 28c the data concavity index is calculated by a statistical segmentation algorithm which binned the S-A data of the channel profiles contiguous to the main stem.

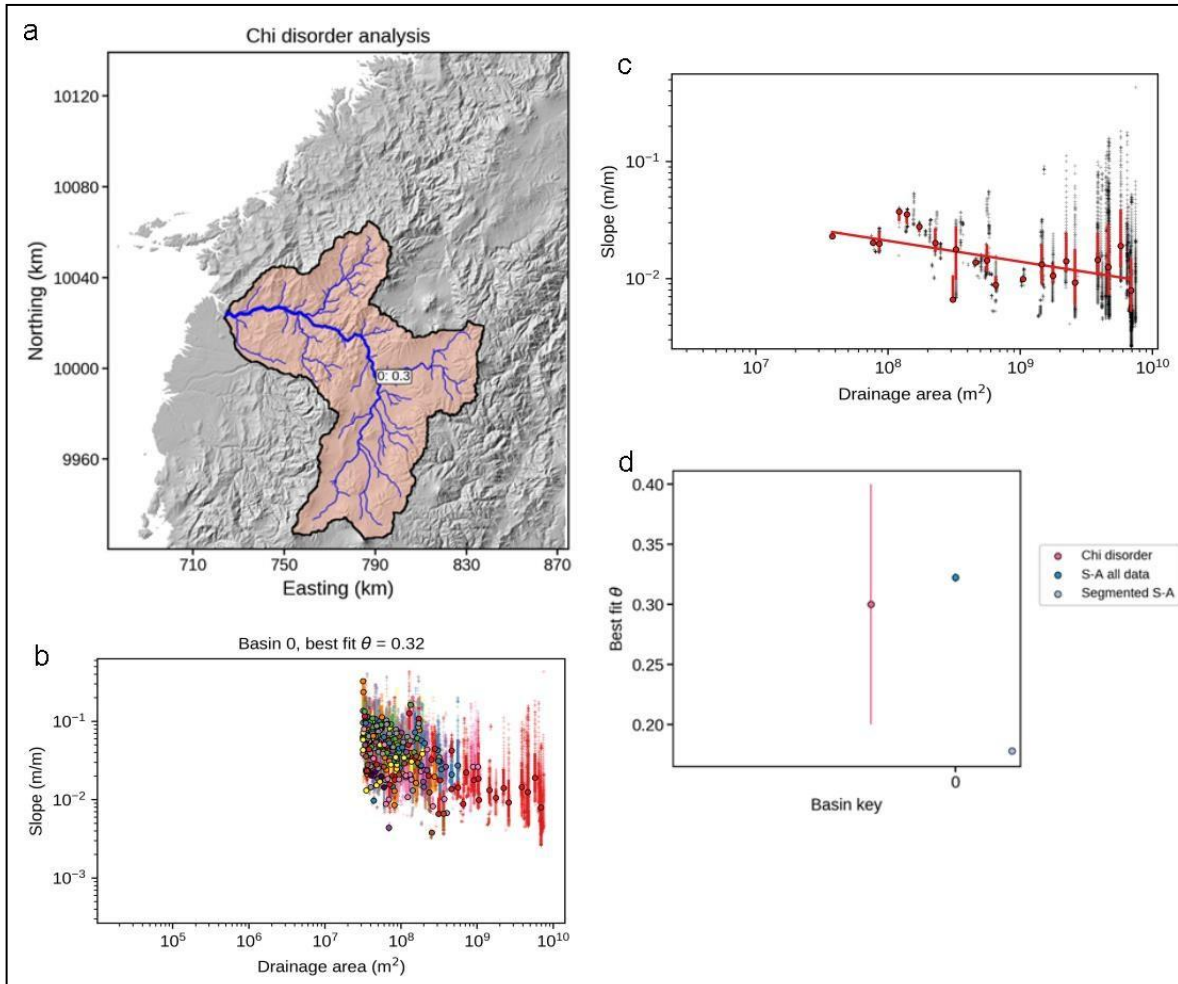


Figure 28. Plots showing the concavity index obtained by a chi disorder (a), of the channel network (b and c). Moreover, the best fit concavity the all methods together (d), the chi methods are colored in red and slope-area methods in blue colors. c) is zoomed of b) where shows the gaps on the slope-area space due to the tributaries joins to the main stem.

In the best fit concavity methods, concavity values from 0.1 to 0.8 are used (Fig. 30), searching for the value that yields the best collinearity of the fluvial network. In this case, the best fit concavity index is 0.3 (Figure 29b) since the tributaries are best co-linearized to the main stem. When the concavity is 0.1 (Figure 29a), the tributaries are steeper than the main stem, while, if the concavity is 0.8 (Figure 29c). the tributaries are shallower than the main stem.

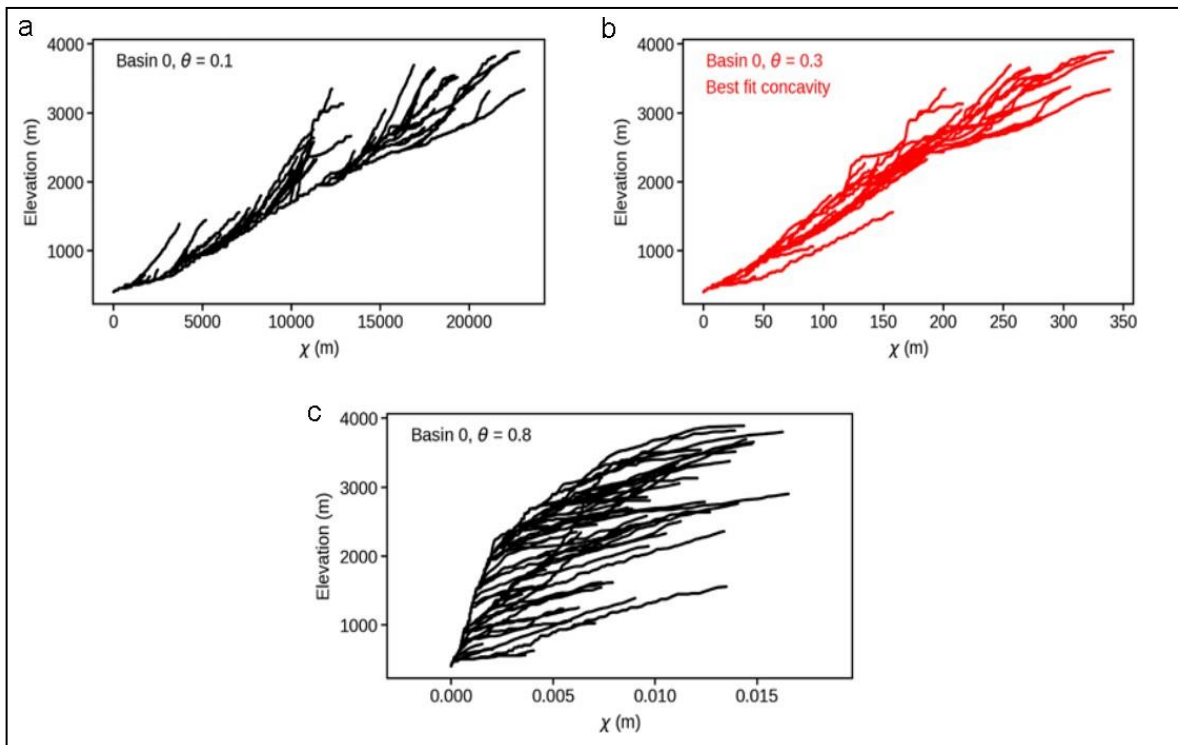


Figure 29. Chi plots for the Guayllabamba basin based on the best fit concavity method. (a) Plot shows the profile with the concavity 0.1. (b) Plot showing the best fit concavity to the basin. (c) Plot shows the profile with the concavity 0.8.

4.2.3.2 Mira basin

The results of the concavity index in the Mira basin are larger in both methods, chi disorder, and slope-area. Thus, the results are 0.4 of concavity for the chi disorder (Figure 30a, e) and 0.35 to the slope-area methods. As in the Guayllabamba basin, the slope-area method clearly shows how much noise is present in the data (Figure 30 b, d). In plot d, the wide dispersion in the data and grouping of the data is clearer to observe.

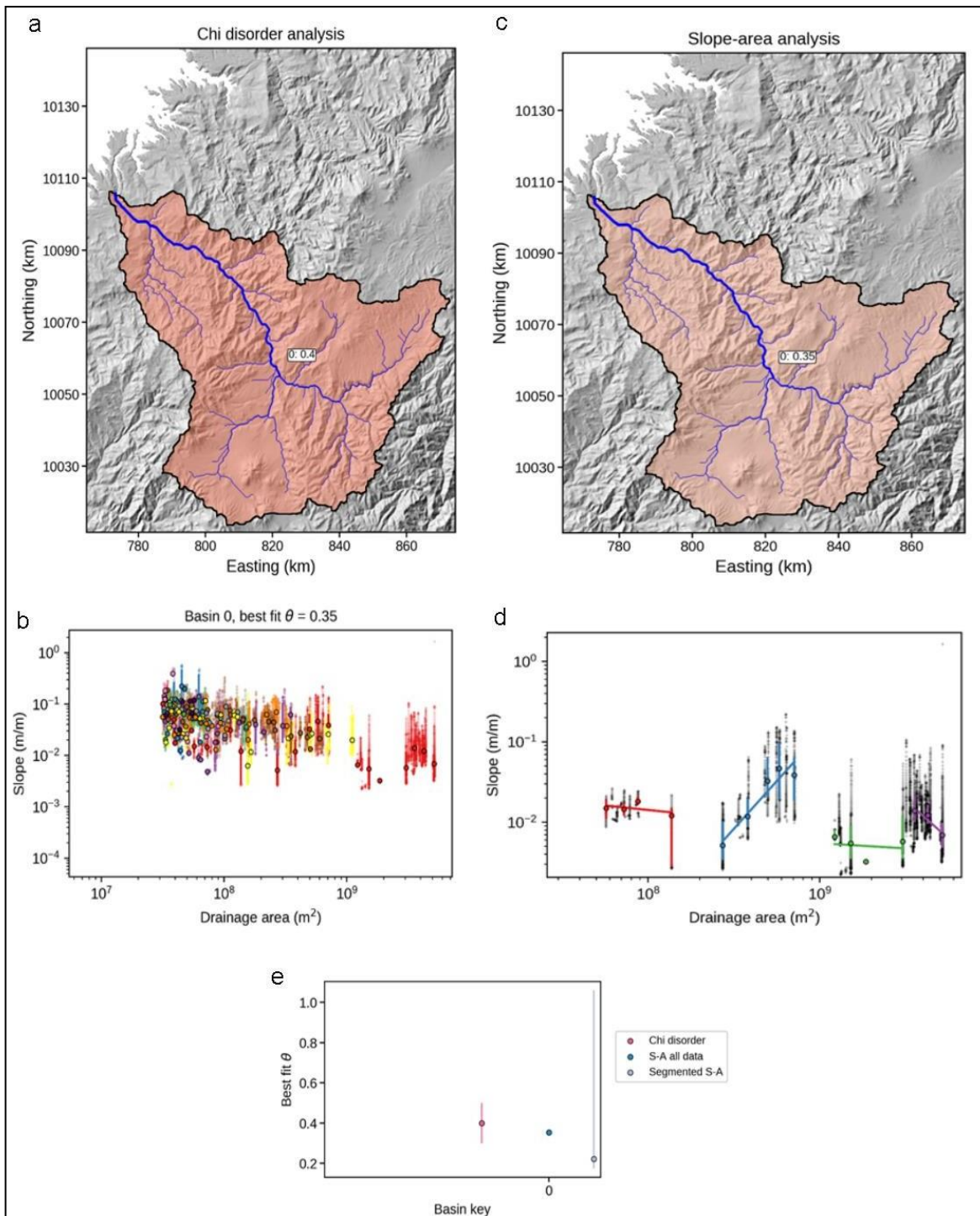


Figure 30. Plots of the Mira basin showing the change in the results of the concavity index obtained depending of the method used, by a chi disorder (a), slope-area (c) of the channel network (b and d), and all the methods binned (e).

The results from the best fit concavity method in the Mira basin are shown in Fig. 31, with values between 0.1 and 0.7. A value of 0.1 results in tributaries that are steeper than the main stem (Figure 31a), while a value of 0.7 results in tributaries that are shallower than the main stem (Figure 31c). The best fit concavity for the chi plot is 0.4 (Figure 31b) because the tributaries are collinear to the main stem.

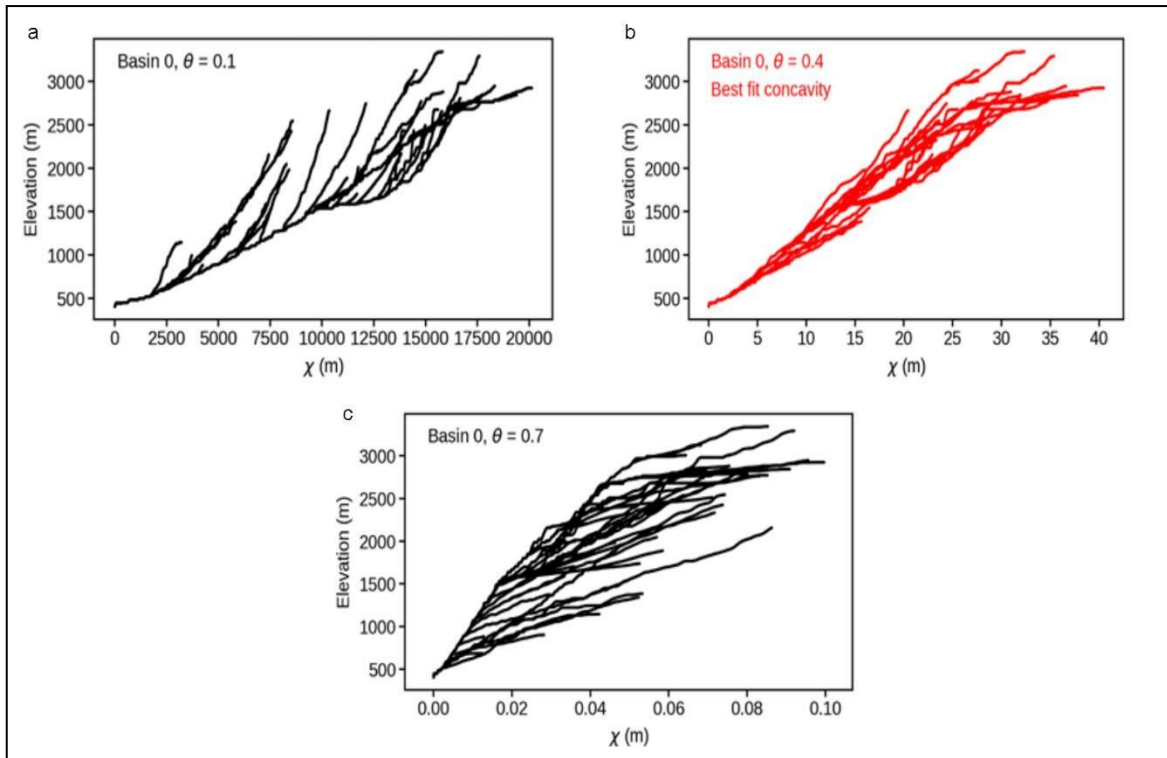


Figure 31. Chi plots for the Mira basin showing the difference on the concavity indices. (a) Plot shows the profile with the concavity 0.1. (b) Plot showing that 0.4 is the best fit concavity to the basin. (c) Plot shows the profile with the concavity 0.7.

4.2.4 Chi plots

The chi plot of the Guayllabamba basin was performed using an $m/n=0.4$, which is a common value for most rivers and is the default value for this parameter in our calculation. In the profile we can observe that there are 4 segments with different steepness index, 0-100m, 100-275m, 275-325m, and 325-400m. It is

clearly observed that the profile does not have a straight line and this means these rivers don't have a singular equilibrium.

For the chi plot of the Mira basin, we use a $m/n=0.2$ to fit tributaries to the main stem. Mira's plot is less co-linear than the Guayllabamba plot, and instead has a concave upward geometry. There is an abrupt change within the main stem and the tributaries at $\sim 1700\text{m}$.

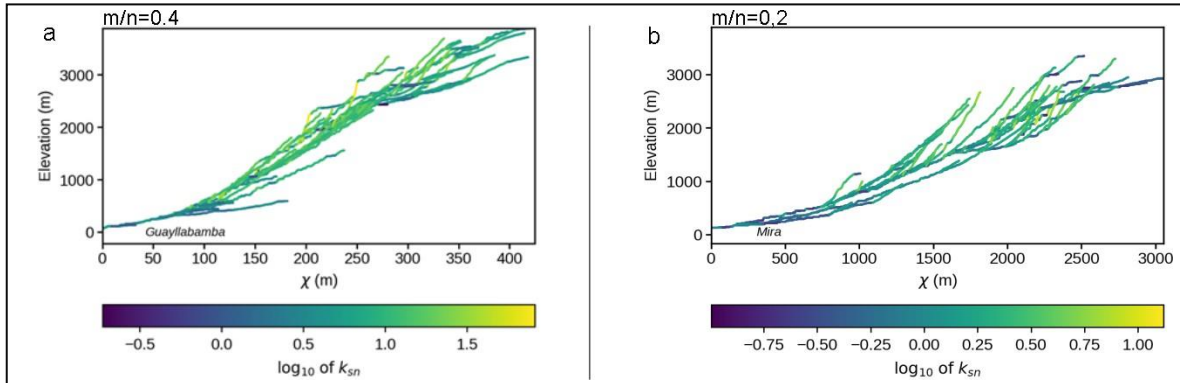


Figure 32. a,b) Chi profiles of the Guayllabamba and Mira Basins colored by the channel steepness.

4.2.5 Steepness plots

The steepness values calculated along the Guayllabamba river are shown on its longitudinal profile (Figure 33a). There are several locations with abrupt changes in steepness that we interpret as knickpoints at 120km, 160km, 220km in the main stem as well as within two tributaries with an abrupt change in their steepness that correspond to knickpoints. The steepness in the Guayllabamba profile is larger upstream, but most of the basin is between 0-1.5. The Mira basin has a steepness index between -0.8 and 0 except in the concave up, where there is a steepness index above the 0.2.

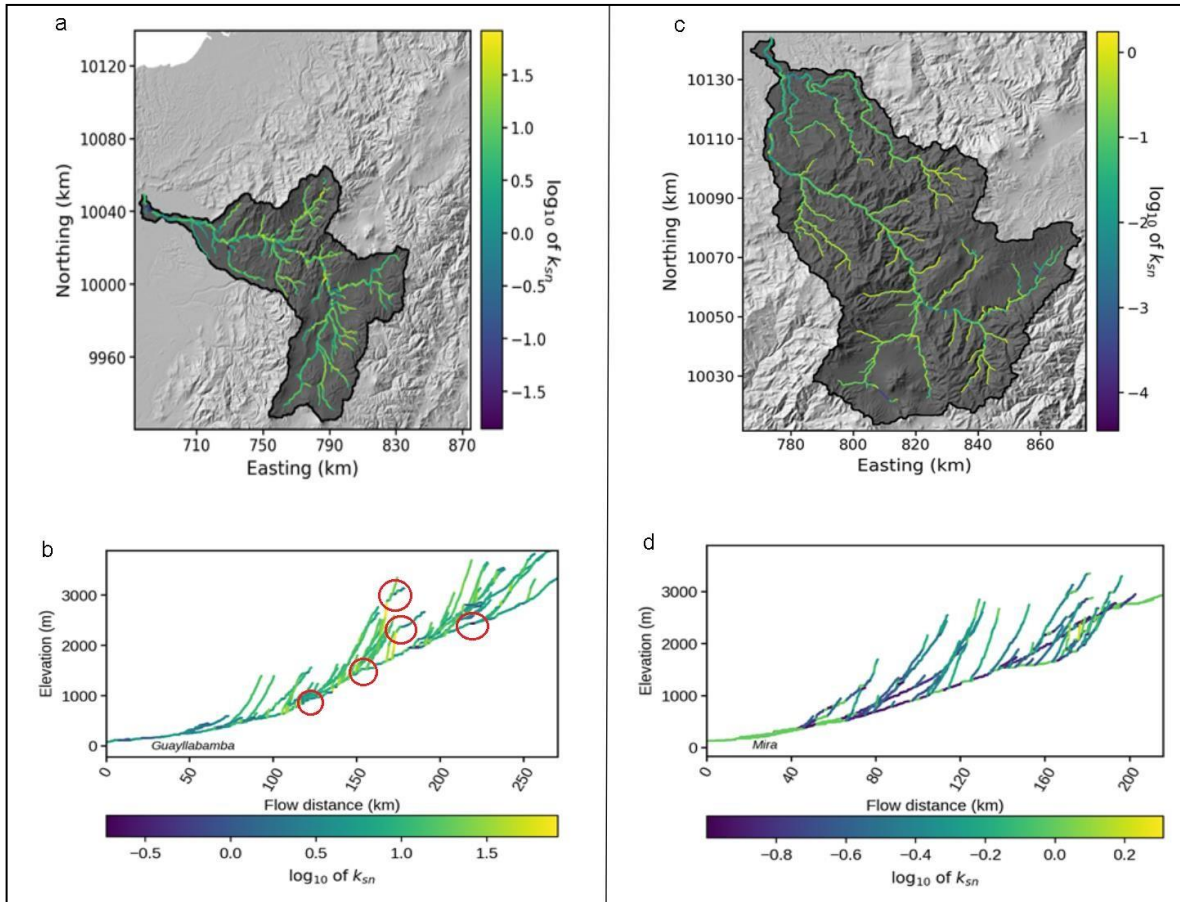


Figure 33. a,c) Maps of the Guayllabamba and Mira Basins with drainage network colored by steepness. Steepness index plots of Guayllabamba (b) and Mira (d) basins. Knickpoints marked with red circle.

5. DISCUSSION

5.1 Terraces, landslides, and scarps

The area of the material removed from the depression is almost the same on both sides of the Pisque river as we can see in the cross-section (Figure 34). In the interpretation of the scarps, it seems to be controlled by the river. The scarps seem to be controlled by the base level of the river. Therefore, the river erodes the material from the bottom to the top, which causes the collapse of the landslides and the formation of scarps.

Moreover, according to the results, comparing the volumes of the area corresponding to the eroded material of the Guayllabamba Depression and the total volume of the fluvial terraces along the Guayllabamba river, near 100% of the material was not stored on the fluvial terraces. This means that the majority of the eroded material from the depression possibly flows to the Pacific or is stored on the fluvial fan of the Los Bancos.

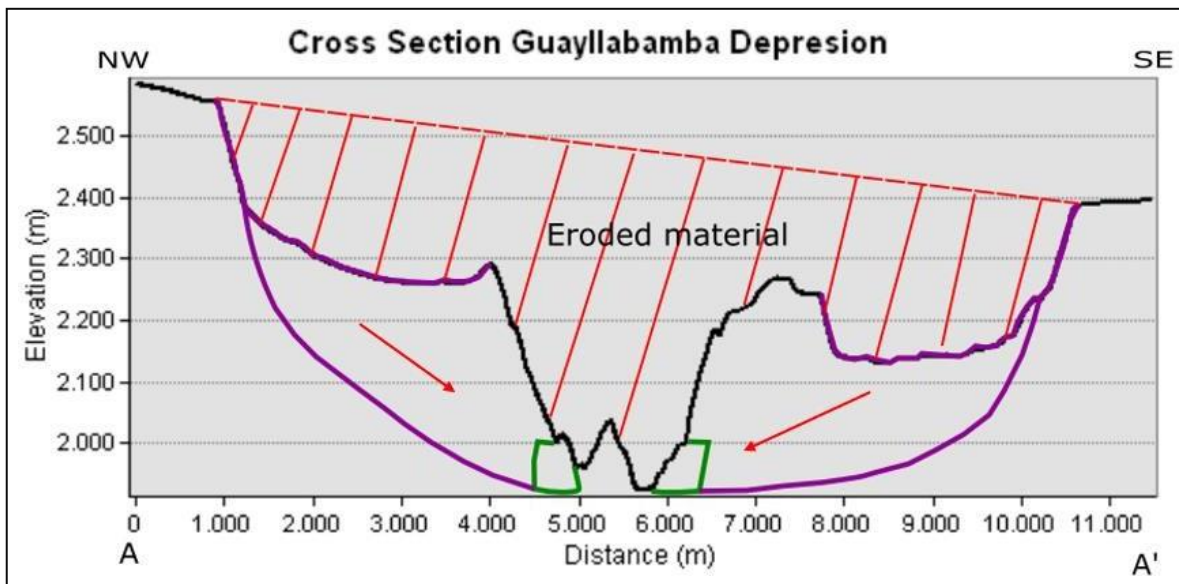


Figure 34. Cross section of the Guayllabamba Depression showing the landslides scarps (purple) and fluvial terraces (green), river channel (black lines), and the area of the eroded material. Location of the cross section in Figure 23.

The topography of the Guayllabamba depression features two large rotational landslides with arcuate escarpments. In addition, the depression presents the fluvial and terrain terraces (Figure 25) belonging to the Pisque river and the respective channel of the river.

5.2 Concavity index

The majority of the bedrock river profiles in steady-state show a concave up shape (Wobus et al., 2006). This is not the case of the Guayllabamba river because the main stem denotes a concave down shape. Moreover, the tributaries before the 150m (Figure 32a) on the chi plot denote a concave up profile, and after that a concave down profile. The best fit concavity index to the Guayllabamba river is 0,3 while the majority of the rivers in tectonically active regions present a high concavity index (Figuroa & Knott., 2010). The same occurs in the Mira basin where the best fit concavity index is 0,4. In the case of the Mira river profile, this presents a concave up shape in the whole river.

5.3 Chi analysis

In the longitudinal profile of Guayllabamba river (Figure 35) its clearer the 4 straight segments which denotes different steepness index. In the first section the steepness index is low and this is due to the river is crossing the coastal plain. The first section shows a concave shape. The steep part has high steepness index which could be interpreted as a section of tectonic uplift, but this part corresponds where the river is crossing the Cordillera Occidental. Moreover, this section shows a concave down shape. The third section is where the Guayllabamba river crosses the Guayllabamba Depression, the profile is straight suggesting no active faults. Furthermore, apparently the Pisque river is not influencing the profile of the Guayllabamba river.

The Mira profile shows tributaries less collinear than Guayllabamba profile. The chi Mira profile also denotes a transient landscape in the main stem and in the majority of its tributaries because also denotes these are not linear.

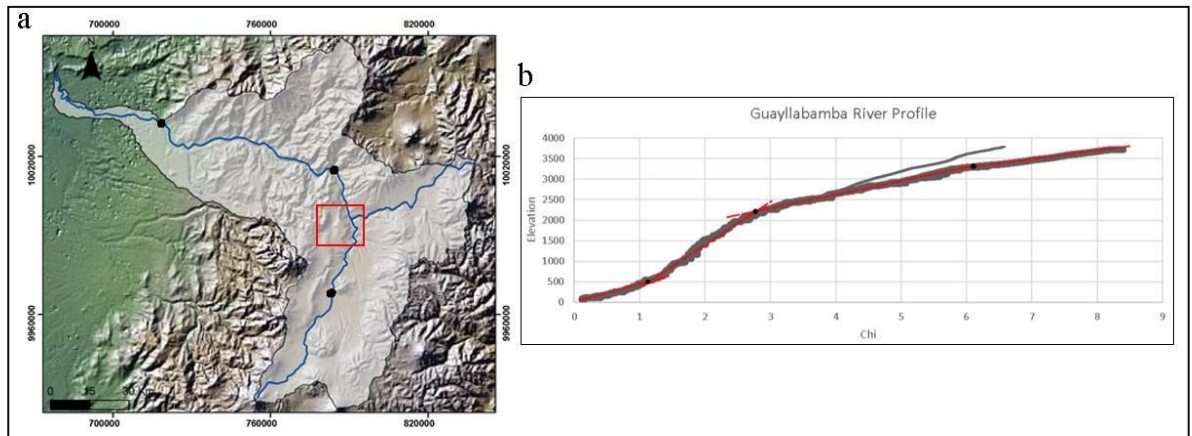


Figure 35. Map of the Ecuador with the Guayllabamba and Pisque rivers (blue). profile of the Guayllabamba river.

5.4 Channel steepness

In the Guayllabamba profile (Figure 33a) knickpoints are not present on the main stem, but are present in two tributaries near the Guayllabamba Depression. These knickpoints are of the slope-break type, characterized by the change of the steepness above and below the knickpoint. The presence of the knickpoints is evidence of rock uplift, however, this can be produced by a tectonic event or can be a product of landslides, variation in rock strengths, river incision, and climate changes (Wobus et al., 2006; Whipple et al., 2013).

On the other hand, the Mira river profile (Figure 33b) shows the presence of two knickpoints on the main stem upstream and some knickpoints along its tributaries. These knickpoints are also of slope-break type, and here the change on the steepness index is more clear than the Guayllabamba profile because it covers a more extensive area due to the influence of the knickpoints in the steepness. The changes in the elevation showing the different reaches in the channel separated by high or low steepness index denote a transient landscape (Wobus et al., 2006).

6. CONCLUSIONS

1. The morphology of the Guayllabamba Depression and the eroded material is symmetric with respect to the river.
2. Using a DEM in ArcGIS, we calculate the volume of the eroded material in the Guayllabamba Depression and the terraces in the Guayllabamba basin, obtaining that the majority of the material missing from the Guayllabamba Depression has not been stored on the fluvial terraces, which mean the river transported the eroded material from the system.
3. The chi and steepness profiles document a steady state landscape along the Guayllabamba Depression and a concave up and down shape where the river crosses the Cordillera. The contrast in the profile of the Mira and Guayllabamba rivers suggest that there is uplift of the Cordillera Occidental at the latitude of Quito but not.
4. Based on the results, the Guayllabamba Depression can be developed solely by river erosion and not by tectonic action.

7. REFERENCES

- Ahmed, M. F., Ali, M. Z., Rogers, J. D., & Khan, M. S. (2019). A study of knickpoint surveys and their likely association with landslides along the Hunza River longitudinal profile. *Environmental earth sciences*, 78(5), 1-15.
- Alvarado, A., L. Audin, J. M. Nocquet, S. Lagreulet, M. Segovia, Y. Font, G. Lamarque, H. Yepes, P. Mothes, F. Rolandone, P. Jarrin, and X. Quidelleur (2014). *Active tectonics in Quito, Ecuador*, assessed by geomorphological studies, GPS data, and crustal seismicity. *Tectonics*, 33(2), 67–83.
<https://doi.org/10.1002/2012TC003224>
- Alvarado, A., Audin, L., Nocquet, J. M., Jaillard, E., Mothes, P., Jarrin, P., ... Cisneros, D. (2016). Partitioning of oblique convergence in the Northern Andes subduction zone: Migration history and the present-day boundary of the North Andean Sliver in Ecuador. *Tectonics*, 35(5), 1048–1065. <https://doi.org/10.1002/2016TC004117>
- Andrade Villafuerte, A. L. (2016). *Análisis de la influencia de la geodinámica y los impactos antropicos en la geomorfología fluvial del río coca. Caso de estudio: impactos fluviales del proyecto Coca Codo SINCLAIR–PHCCS*. Bachelor thesis, Escuela Politecnica Nacional, Quito, Ecuador.
- Aspden, J. A., Litherland, M., & Salazar, E. (1988). UM interpretación preliminar de la historia colisional del Centro y Sur del Ecuador y posibles controles para la geología cenozoica y de mineralización polimetálica. *Politecnica, Monografía de Geología*, 6, 49-75.
- Aspden, J. A., & Litherland, M. (1992). *The geology and Mesozoic collisional history of the Cordillera Real, Ecuador*. *Tectonophysics*, 205(1-3), 187-204.
- Egholm, D. L., Knudsen, M. F., & Sandiford, M. (2013). Lifespan of mountain ranges scaled by feedbacks between landsliding and erosion by rivers. *Nature*, 498(7455), 475-478.
- Ego F., Sebrier M. (1996), The Ecuadorian Inter-Andean Valley: a major and complex restraining bend and compressive graben since Late Miocene Time. *Annales Tectonicae*, Vol X No. 12. pp. 31-59.
- Ely, C. P. (2017). *A Geomorphic Characterization of an Ecuadorian Paramo River* (Doctoral

dissertation, Appalachian State University).

Figuerola, A. M., & Knott, J. R. (2010). Tectonic geomorphology of the southern Sierra Nevada Mountains (California): Evidence for uplift and basin formation. *Geomorphology*, *123*(1-2), 34-45.

Gregory, K.J., 2000. *The Changing Nature of Physical Geography*. Arnold, London.

Gutierrez, M. (2008). Geomorfología. En *Geomorfología Fluvial I y II* (págs. 275-348). Madrid: Pearson Prentice Hall.

Gutscher, M. A., Malavieille, J., Lallemand, S., & Collot, J. Y. (1999). Tectonic segmentation of the North Andean margin: impact of the Carnegie Ridge collision. *Earth and Planetary Science Letters*, *168*(3-4), 255-270.

Hughes, R. A., & Pilatasig, L. F. (2002). *Cretaceous and tertiary terrane accretion in the Cordillera Occidental of the Andes of Ecuador*. *Tectonophysics*, *345*(1-4), 29-48.

Korup, O., Clague, J. J., Hermanns, R. L., Hewitt, K., Strom, A. L., & Weidinger, J. T. (2007). Giant landslides, topography, and erosion. *Earth and Planetary Science Letters*, *261*(3-4), 578-589.

Litherland, M; Aspden, A; Jemielita, R. (1994). *The metamorphic belts of Ecuador*.

Marliyani, G. I., Arrowsmith, J. R., & Whipple, K. X. (2016). Characterization of slow slip rate faults in humid areas: Cimandiri fault zone, Indonesia. *Journal of Geophysical Research: Earth Surface*, *121*(12), 2287-2308.

Menendez, I., Silva, P.G., Martin-Betancor, M., Pérez-Torrado, F.J., Guillou, H., Scaillet, S., 2008. Fluvial dissection, isostatic uplift, and geomorphological evolution of volcanic islands (Gran Canaria, Canary Islands, Spain). *Geomorphology* *102*, 189-203.

Michaud, F., Witt, C., & Royer, J. Y. (2009). Influence of the subduction of the Carnegie volcanic ridge on Ecuadorian geology: Reality and fiction. *Memoir of the Geological Society of America*, *204*(December 2014), 217-228.

Mudd, S. M., Attal, M., Milodowski, D. T., Grieve, S. W., & Valters, D. A. (2014). A statistical framework to quantify spatial variation in channel gradients using the integral method of channel profile analysis. *Journal of Geophysical Research: Earth Surface*, *119*(2), 138-152.

- Mudd, S. M., Clubb, F. J., Gailleton, B., & Hurst, M. D. (2018). How concave are river channels? *Earth Surface Dynamics*, 6(2), 505-523.
- Mudd, S. M., Clubb, F. J., & Gailleton, B. (2018, August 28). *User guide to chi analysis*. https://lsdtopotools.github.io/LSDTT_documentation/LSDTT_chi_analysis.html
- Niemann, J. D., Gasparini, N. M., Tucker, G. E., & Bras, R. L. (2001). A quantitative evaluation of Playfair's law and its use in testing long-term stream erosion models. *Earth Surface Processes and Landforms: The Journal of the British Geomorphological Research Group*, 26(12), 1317-1332.
- Nocquet, J. M., Villegas-Lanza, J. C., Chlieh, M., Mothes, P. A., Rolandone, F., Jarrin, P., ... & Yepes, H. (2014). Motion of continental slivers and creeping subduction in the northern Andes. *Nature Geoscience*, 7(4), 287-291.
- Nuñez, C. (2011). *Geología del cuaternario y geomorfología tectónica entre Villadora y Bellavista, río Guayllabamba*. Tesis de grado, Escuela Politecnica Nacional. Quito, Ecuador.
- Paez Molineros, J. A. (2019). *Análisis de terrazas fluviales en el río Guayllabamba, sector Perucho, provincia de Pichincha*. Bachelor thesis, Escuela Politecnica Nacional. Quito, Ecuador.
- Perron, J. T., & Royden, L. (2013). An integral approach to bedrock river profile analysis. *Earth Surface Processes and Landforms*, 38(6), 570-576.
- Reyes, P. S., Valarezo, M. E., Córdova, J., Michaud, F. A., & Zapata, C. (2018). Quantitative morphometric analysis of the Jama River profile in a tectonically active margin (Northwestern Ecuador). *Journal of Mountain Science*, 15(5), 966-975.
- Spikings, R. A., Seward, D., Winkler, W., & Ruiz, G. M. (2000). *Low-temperature thermochronology of the northern Cordillera Real, Ecuador: Tectonic insights from zircon and apatite fission track analysis*. 19(4), 649–668.
- Spikings, R. A. (2005). *Thermochronology of the Cordillera Occidental and the Amotape Complex, Ecuador: unraveling the accretionary and post-accretionary history of the Northern Andes*.
- Tarback, E. J., Lutgens, F. K., & Tasa, D. (2005). Surface water currents. *Earth Sciences an*

Introduction to Physical Geology (pg. 451).

- Tibaldi A., Ferrari L. 1992, From latest Miocene thrusting to Quaternary transpression and transtension in the Interandean Valley, Ecuador. *Journal Geodynamics*, Vol 15, No. 1/2, pp. 59-83.
- Thorndycraft, V. R., Benito, G., & Gregory, K. J. (2008). Fluvial geomorphology: A perspective on current status and methods. *Geomorphology*, 98(1-2), 2-12.
- Vallejo, C. (2007). *Evolution of the western cordillera in the Andes of Ecuador (late cretaceous Paleogene)*. PhD Thesis, ETHZ, Zürich, Switzerland.
- Vallejo, C., Winkler, W., Spikings, R. A., Luzieux, L., Heller, F., & Bussy, F. (2009). *Mode and timing of tectonic accretion in the forearc of the Andes in Ecuador. Backbone of the Americas: shallow subduction, plateau uplift, and ridge and terrane collision*, 204, 197.
- Villagomez, D. (2003). Evolución geológica plio-cuaternaria del Valle Interandino central en Ecuador. Bachelor thesis, Escuela Politécnica Nacional. Quito, Ecuador.
- Whipple, K.X., DiBiase, R.A., Crosby, B.T., 2013. Bedrock rivers. In: Shroder, J. (Editor in Chief), Wohl, E. (Ed.), *Treatise on Geomorphology*. Academic Press, San Diego, CA, vol. 9, Fluvial Geomorphology, pp. 550–573.
- Whittaker, A. C., Attal, M., Cowie, P. A., Tucker, G. E., & Roberts, G. (2008). Decoding temporal and spatial patterns of fault uplift using transient river long profiles. *Geomorphology*, 100(3-4), 506-526.
- Wobus C, Whipple KX, Kirby E, Snyder N, Johnson J, Spyropolou K, Crosby B, Sheehan D. 2006. *Tectonics from topography: procedures, promise, and pitfalls*. In *Tectonics, Climate, and Landscape Evolution*, Willett SD, Hovius N, Brandon MT, Fisher DM (eds), Geological Society of America Special Paper 398, Penrose Conference Series. Geological Society of America: Boulder, CO; 55–74.